Status of thesis

Title of thesis	Wireline Pore Pressure Estimation Study in Carbonate Setting: Case Study on the Eastern Central Luconia Province, Sarawak

I **AZWA JANNAH ABU BAKAR**

Hereby allow my thesis to be placed at the Information Resource Centre (IRC) of University Teknologi PETRONAS (UTP) with the following conditions:

1. The thesis becomes the property of UTP.
2. The IRC of UTP may make copies of the thesis for academic purposes only.
3. this thesis is classified as

	Confidential
X	Non-confidential

If this thesis is confidential, please state the reason: N/A

The contents of the thesis will remain confidential for _____years.

Remarks on disclosure:

Endorsed by

Level 23, PETT 2, KLCC
Date: 14/1/08

Level 4, Block C, PRSB
Date: 14/1/08

UNIVERSITY TEKNOLOGI PETRONAS

Approval by Supervisor (s)

The undersigned certify that they have read, and recommend to The Postgraduate Studies Programme for acceptance, a thesis entitled "**Wireline Pore Pressure Estimation Study in Carbonate Setting: Case Study on the Eastern Central Luconia Province, Sarawak**" submitted **by Azwa Jannah Abu Bakar** for the fulfillment of the requirements for the degree of MSc Petroleum Geoscience.

_____

Date:

Signature : _____

Main Supervisor : DR JAMAAL HOESNI

Date : 14/1/08.

Co- Supervisor : _____

TITLE PAGE

UNIVERSITY TEKNOLOGI PETRONAS

Wireline Pore Pressure Estimation Study in Carbonate Setting: Case Study on the Eastern Central Luconia Province, Sarawak

By

Azwa Jannah Abu Bakar

A THESIS

SUBMITTED TO THE POSTGRADUATE STUDIES PROGRAMME

AS A REQUIREMENT FOR THE

DEGREE OF MSC

PETROLEUM GEOSCIENCE

BANDAR SERI ISKANDAR,

PERAK

DECEMBER, 2007

I hereby declare that the thesis is based on my original work except for quotations and citations which have been duly acknowledged. I also declare that it has not been previously or concurrently submitted for any other degree at UTP or other institutions.

Signature : 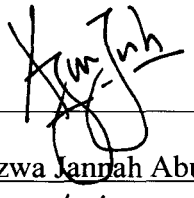

Name : Azwa Jannah Abu Bakar

Date : 14/1/08

TO MY LATE MOM

& FAMILY

Acknowledgements

This research involved many individuals and organizations that supporting and giving their hands to help me to accomplish this report. I want to take this opportunity to thank them.

First of all, my deepest gratitude is toward PETRONAS for financial support and releasing data for this research.

Secondly to my supervisors Dr Jamaal Hoesni and Mr Hamdan Mohamad, not to be forgotten Dr Azlina Anuar for their support, teaching, advising, helping, coaching and mentoring during the four month research.

Next is to PETRONAS Research Sdn. Bhd. (PRSB) and PETRONAS Management Unit (PMU) for the data handling, equipment and facilities that have been used.

Also thanks to my housemates, and also my colleagues in the pioneer batch of UTP-IFP MSc Petroleum Geoscience 2006/2007.

Finally, I would like to thank my family for their moral support when I lost my hope. Thank you so much to all.

Abstract

The pore pressure prediction of clastic sediments using traditional methods, such as Eaton and Miller have been widely used in the oil and gas industry, especially when the excess pressure is related to the disequilibrium compaction. These traditional methods rely on the association of porosity with pressure buildup. Porosity or compaction trend is generally predictable for the clastics. However, the compaction trend is not so obvious in carbonate due to diagenesis and dissolution occurring in the carbonates.

Three methods involving two different equations from Eaton and Miller, using sonic and resistivity curves, were tested to see whether these methods can be applied to the carbonate environment. The three methods are, the 'pore pressure Miller's equation using NCT calculated from the Miller's equation', the second method are the 'Eaton's pore pressure equation using the visualized freehand drawn NCT on resistivity curve' and the third method is the 'pore pressure calculation using the visualized freehand drawn NCT using the Sonic curve'. From the analysis the best method that can be used was the Eaton method on sonic curves.

In the second phase of the analysis, the pressure contribution factor was tested using the basin modeling. Results from the modeling indicated that both thermal and fluid flow as minor pressure contributors in addition to the disequilibrium compaction from sedimentary loading.

Table of Contents

List of Figures

List of Tables

Chapter 1:
Introduction

1.1 Background

This report was done to part one of the requirements of MSc Petroleum Geoscience's course by Universiti Teknologi Petronas (UTP) in collaboration with Institut Francais du Petrole (IFP). This study was conducted to analyze the suitability of the traditional method (Eaton, Miller, Bower etc.) used in the prediction of clastic sedimentary basin pore pressure for carbonates. The parameters used were also investigated to see the variation of the method towards the suitability in terms of the study area compared to the other basins.

The study was divided into two phases. The main aim of the first phase is to predict the pore pressure in the shale above the carbonate and using the method to then predict the pore pressure in the shale between the carbonate. This method was done by assuming that shale within the carbonate is in the equilibrium with the carbonate itself. The second phase objectives are to understand the pressure evolution in the basin and the effect of thief sand toward the pressure evolution.

1.1.1 Pore Pressure Prediction

There are several ways to predict formation pressure. These methods are divided into three groups according to the different stages during exploration. The three groups are Pre Drill, While Drilling and Post Drill (Fig. 1.1).

The pre drill group consists of seismic method, nearby wells, analogy and basin modeling. In the seismic method, the pressure is predicted using velocity data. Normally, in over pressured zones, the sediments are not well compacted. Therefore in the seismic section, we observed a velocity drop in the overpressured. This interpretation can be supported by nearby well data. Nearby wells will have the drilling history that can be used in the pressure prediction study. In basin modeling, several parameters were used to predict the pressure. These include the stratigraphic data, temperature data, vitrinite reflectance, pressure data, etc. All the parameters were combined to run the simulation and reconstruct the over pressure evolution in the basin.

The second group, that is While Drilling, can measure the pressure through drilling rate, Measuring/Logging While Drilling (MWD/LWD) tools, kicks, mud gas, background gas, connection and trip gas, gas analysis, etc. When the depth increases, normally the sediment will become more compacted and the density becomes higher. In other words, the rock becomes harder, thus the drilling rate reduces with depth. Sudden change in the drilling rate, i.e. the drilling rate becomes faster, indicates the possibilities of either a facies change or an undercompacted zone due to occurrence of overpressure. The MWD/LWD tools will give the Gamma Ray, Resistivity and caliper readings. These measurements will help to estimate pressure through software for example Predict Drillwork software. This approach is more accurate compared to wireline measurement since measurement was done during drilling when the formation was relatively less contaminated with the drilling fluid. However wireline measurements are often used because of the wide variety of measurements compared to MWD/LWD, such as the density curve, the neutron porosity curve etc.

The third group is the post drill prediction. Generally, it is done using calculation using either Eaton or Miller's method.

Better pore pressure prediction can be achieve through combination of the three groups, with that it will help the planning of future exploration wells.

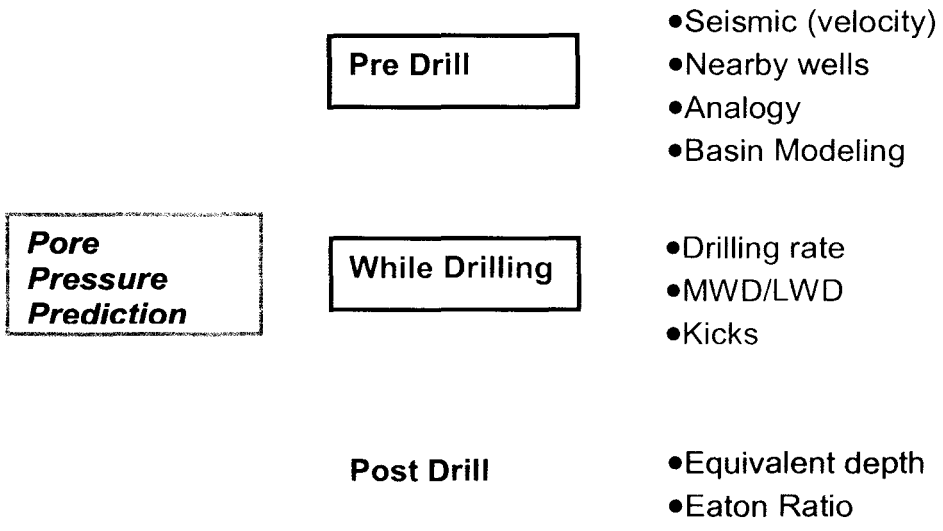

Fig. 1.1 Various ways of predicting pore pressure.

1.1.2 Overpressure Mechanisms

The overpressure mechanisms can be grouped into three broad categories, based on the processes involved: (1) ineffective volume reduction due to imposed stress (vertical loading during burial, lateral tectonic processes) leading to disequilibrium compaction, (2) volume expansion, including porosity increases, due to changes in the solid to liquid ratios of the rock, and (3) hydraulic head and hydrocarbon buoyancy (Fig. 1.2). Disequilibrium compaction results from rapid burial (high sedimentation rates) of low permeability rocks such as shales, and is characterized on pressure vs. depth plots by a fluid retention depth where overpressure commences, and increases downwards along a gradient which can closely follow the lithostatic (overburden) gradient (Swarbick and Osborne, 1998).

The overpressure always represented by pressure vs. depth plot where it contains hydrostatic line, lithostatic line and pore pressure line (Fig. 1.3). From the plotted line, the effective stress and overpressure zone can be illustrated.

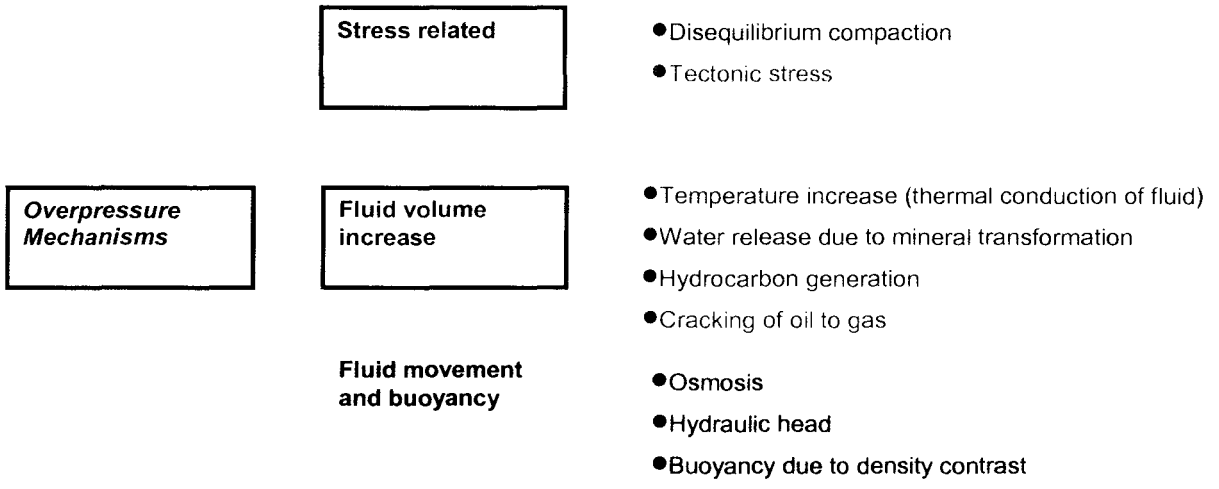

Fig. 1.2 Overpressure mechanisms.

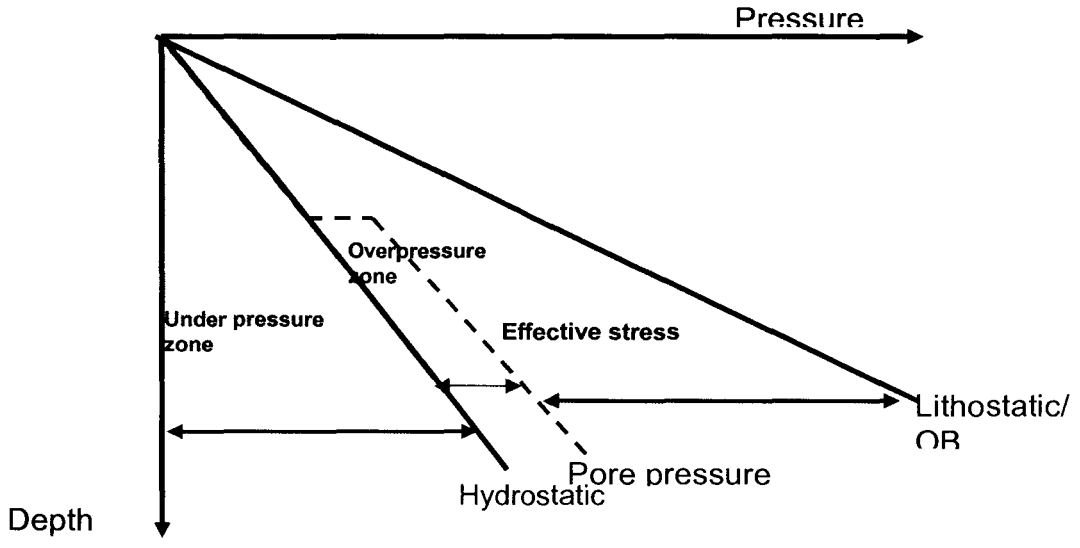

Fig. 1.3 Pressure vs. Depth plot with lithostatic and hydrostatic line that indicate the overpressure and underpressure zones.

1.2 Problem Statement

Pore pressure estimation from wireline logs best suit clastic sedimentary basins, especially when excess pressure is due to disequilibrium compaction. This is because the methods, such as Eaton, rely on the association of porosity with pressure buildup while porosity or compaction trends are generally predictable for clastics. However, for carbonates the compaction trend is less predicted. This is due to the secondary diagenesis and dissolution as a result of pressure solution. The use of the Eaton method has been less successful in carbonate environments.

1.3 Objectives

The objectives of the study are to determine the suitability of traditional pore pressure estimation methods in a carbonate setting and to model the overpressure within the carbonate using 2D basin modeling.

1.4 Scope of Work

The first phase is to derive the normal compaction trend (NCT) in the shale above the carbonate. The shale within the carbonate is assumed to be in equilibrium with the carbonates. By predicting the NCT, the zone with the under compaction zone can be predicted and can be assume to have overpressure above the hydrostatic line. The NCT in the shale above is then tested whether it can be applied in the shale between the carbonate. This attempt is done by using the Drillwork Predict software.

The second phase is the Temis 2D basin modeling software to help construct the overpressure evolution in the basin.

Chapter 2
Study Area

2.1 Location

The study area is situated in the Eastern Central Luconia Province, offshore Sarawak. Areally it is approximately 10, 175km^2 (110km x 92.5km; Fig. 2.1) with water depths ranging from 70m to 114m. The main reservoirs here are carbonates of Miocene age.

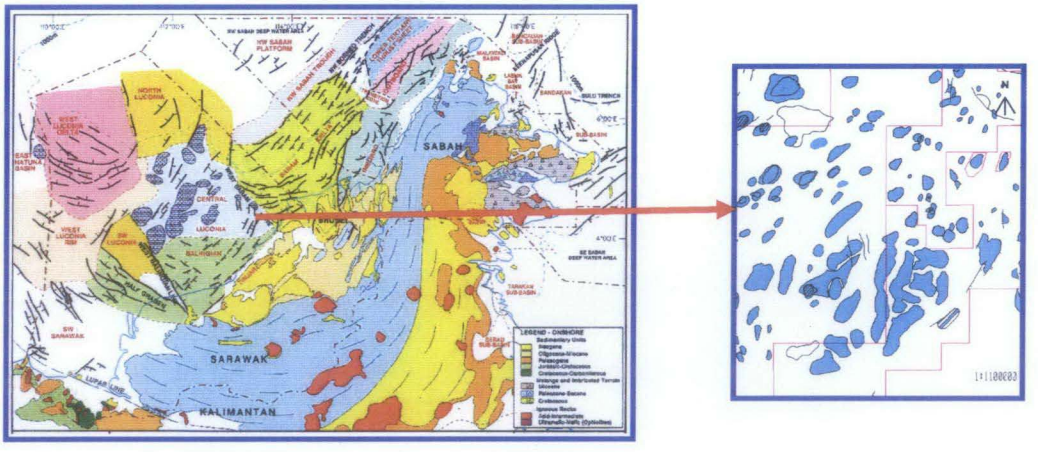

Fig. 2.1 Location of the study area and highlighted in the smaller blue box to view the carbonates in the area.

2.2 Geological setting

2.2.1 Structural Elements

The Central Luconia Province is located between an extensional area in the north and a compressive area in the south. During the Oligocene to the Middle Miocene, sea floor spreading affected the continental crust to the south. The deepening of South China Sea and the opening to the southwest allowed marine currents to supply large amounts of nutrientrich water to the Sarawak shelf and enabled the extensive growth of Middle Miocene to Late Miocene carbonate buildups. The evolution of the Sarawak Basin from Cycle I to Cycle IV shows how sediment was brought into the basin and how the coast line changed with time (Fig. 2.2).

Crustal extension in the Central Luconia caused the development of horsts and grabens that control the size and distribution of buildups (Fig. 2.3). Large carbonate buildups develop on highs while pinnacletype carbonates develop within the basinal area where subsidence is stronger and closer to the source of clastic material. The development of some of the buildup was also controlled by the re-activation of thrust faults that occur during carbonate deposition. The southwest-northeast alignment of the buildups, especially in the central and eastern part, probably reflects rift-induced structural trends.

The Central Luconia Province has undergone several episodes of structural deformation. The dominant structural feature in the southern part of Central Luconia is the central ridge, which trend NNE-SSW and plunges gently to the NNE, as a series of tilted fault blocks (Ali and Abolins, 1999).

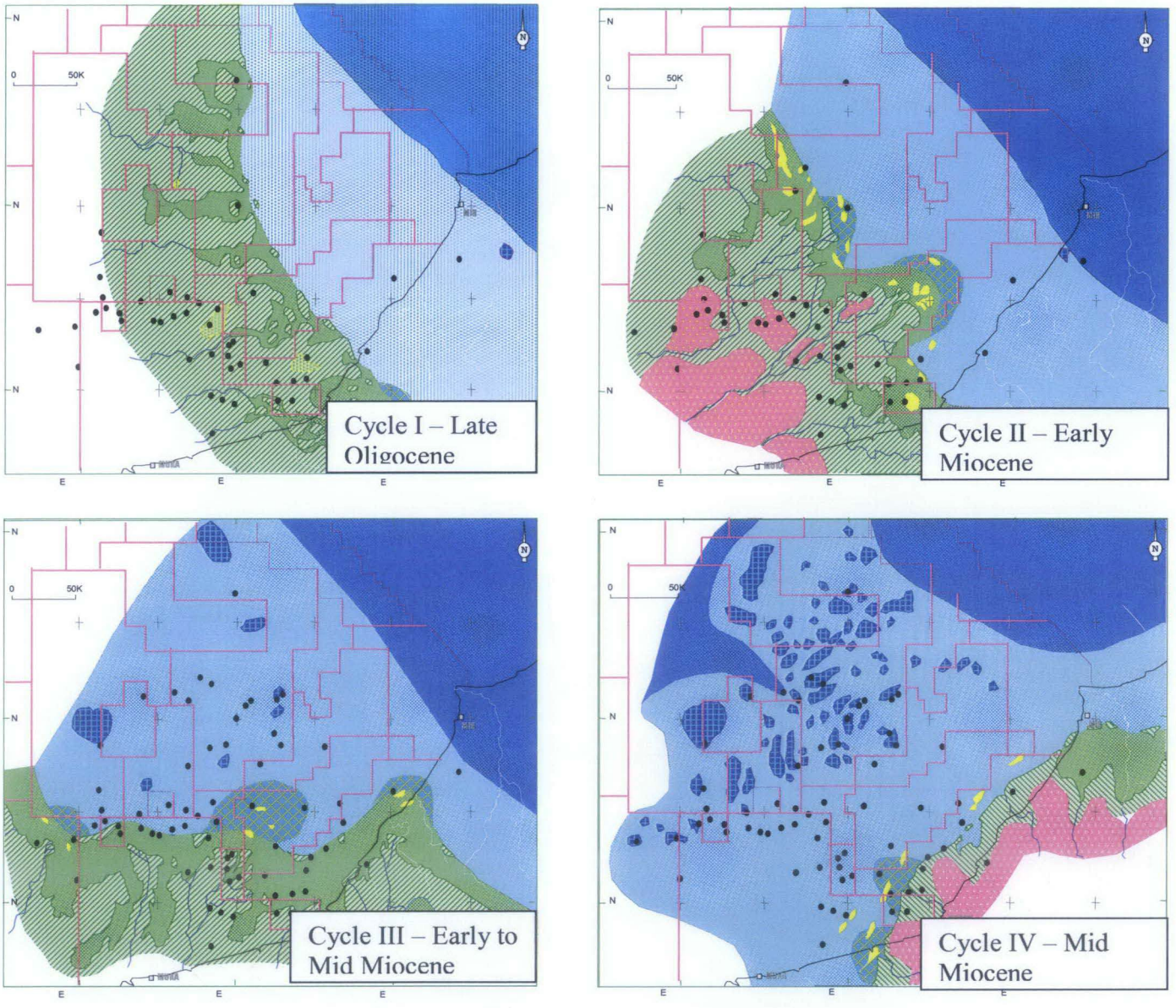

Fig. 2.2 Paleogeographic map of Sarawak showing the evolution from Cycle I up to Cycle IV. The coastline moved from the west to the southeast. The carbonates started to develop in Early Cycle III and extensively grew in the late Cycle III. (modified after Idris et. al. 2005).

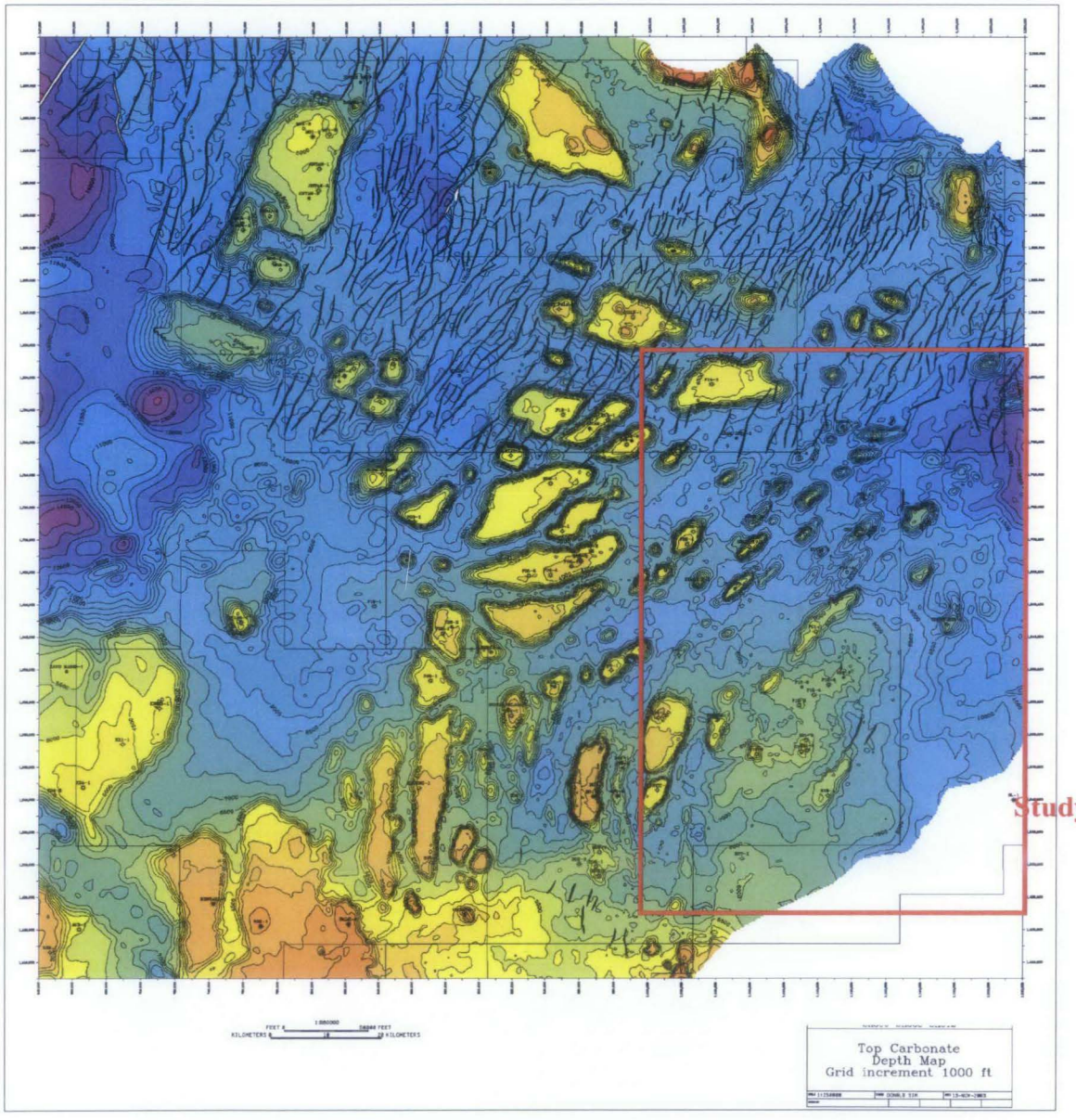

Fig. 2.3 The distribution of carbonate buildups in the Central Luconia (after SSB, 2007).

2.2.2 Stratigraphic Elements

The Central Luconia Province has undergone several episodes of sedimentation. A number of individual structural elements had long-lived effects on sedimentation on the platform, and have directly affected the geometry of the pre-carbonate siliciclastics, the carbonate buildups and the overlying siliciclastics. During Cycle I, the area underwent an early synrift graben fill whereby deepwater argillaceous and shallow marine siliciclastic succession were deposited. This was followed by a late phase of synrift sedimentation throughout Cycles II and III during the opening of the South China Sea. Continuous subsidence and formation of half-grabens resulted in widespread Middle to Upper Miocene carbonate depositon during Cycles IV and V. This was eventually terminated by the influx of siliciclastics sediments derived from the uplifted Rajang Fold-Thrust Belt during Cycles V to VIII (Fig. 2.4).

Carbonate deposition in the Central Luconia Province started during the Early Miocene (Late Cycle III times) and continued until the present day in deeper water areas. Most of the Cycle III carbonates were deposited as localized discontinuous banks that became tight argillaceous limestone stringers encased in siliciclastic sediments. During Cycles IV and V times, carbonate production exceeded siliciclastic deposition within the Central Luconia Province, resulting in the deposition of extensive carbonate buildups (Ali and Abolins, 1999).

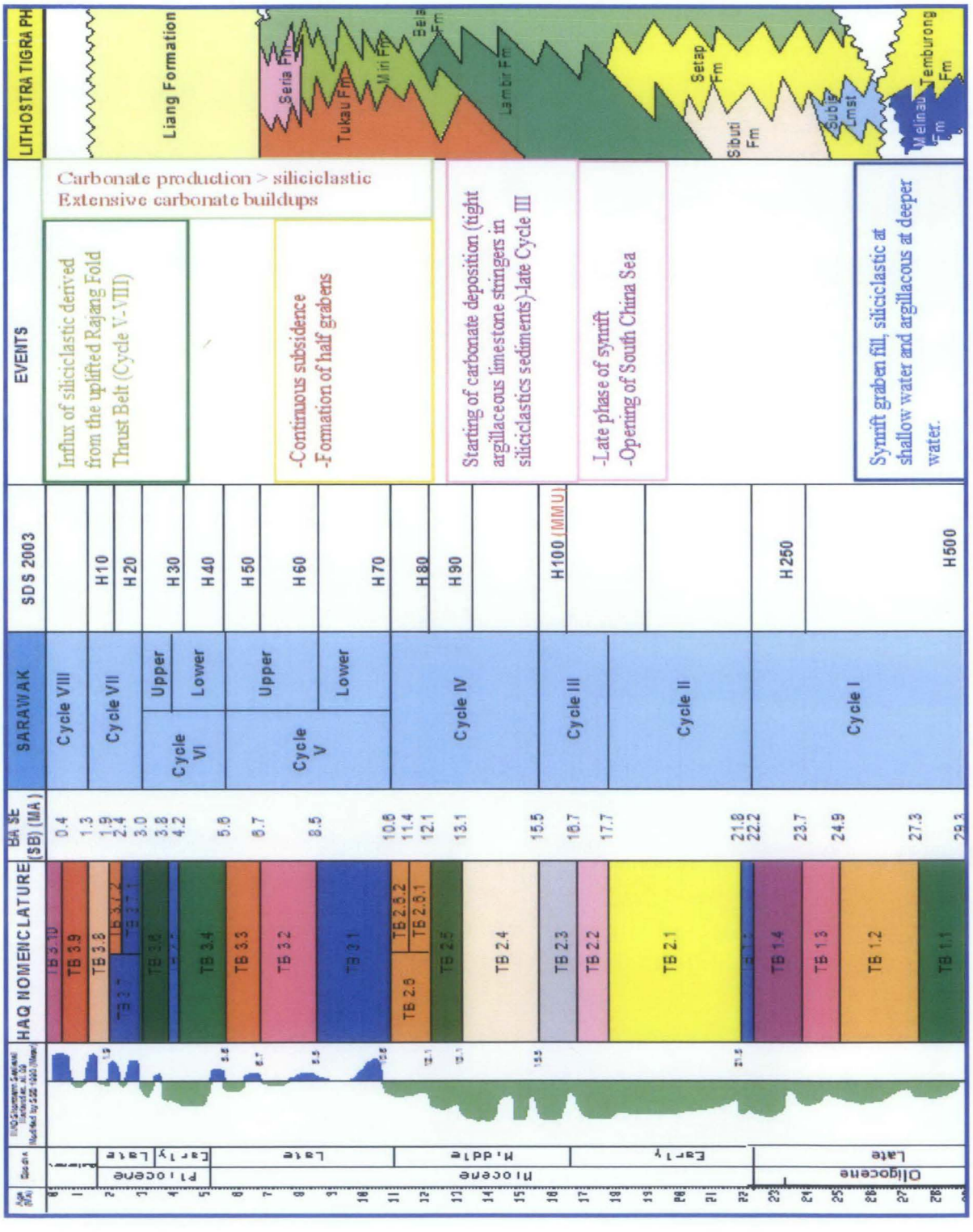

Fig. 2.4 Summary of events in the Central Luconia Province through time (modified after SSB 1998).

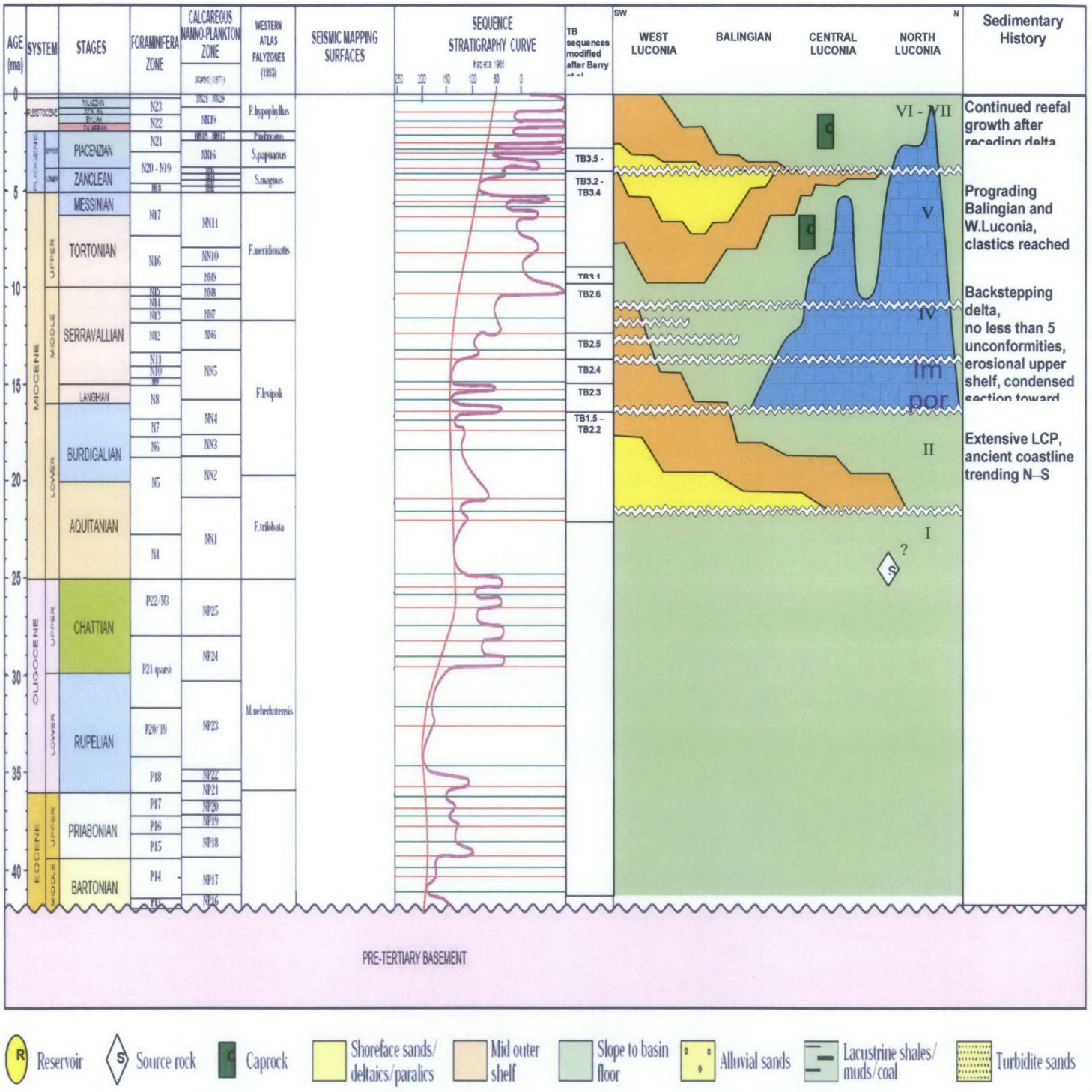

Fig. 2.5 Stratigraphic chart showing the base of carbonate in Cycle III and the top of carbonate in Cycle V in the Central Luconia Province (modified after Barry 2005).

2.3 Overpressure Setting

The prediction of pore pressure (PP) is primarily established based on the divergence of petrophysical measurements from the normal compaction trend. In the transition zone between the hydrostatically pressured and geopressured systems, formation water is expelled gradually from the sediments due to the pressure gradient drop from deeper to shallow depth. In this transition zone, velocity, density, and resistivity increase downward concurrent with the rate of dewatering process. The normal compaction trend represents the optimum fitted linear trend of these measured data in the low permeable beds in this transition zone. Conversely, in a geopressured system (where water is no longer capable of escaping), velocity, density, and resistivity measurements decreased in the low permeable beds (Shaker, 2007).

A study has been carried out by Sarawak Shell Sdn Bhd. and they found that in the Central Luconia province, there are roughly three areas that can be grouped according to overpressure conditions (pers. comm: Van Vliet, A., 2007). The groups are, extremely high overpressure (1322psi-1372psi above the hydrostatic pressure), high overpressure (287psi-316psi above the hydroststic pressure) and mildly overpressure (40psi-200psi above the hydrostatic pressure). The study area falls mostly in the mildly overpressured area (Fig. 2.6).

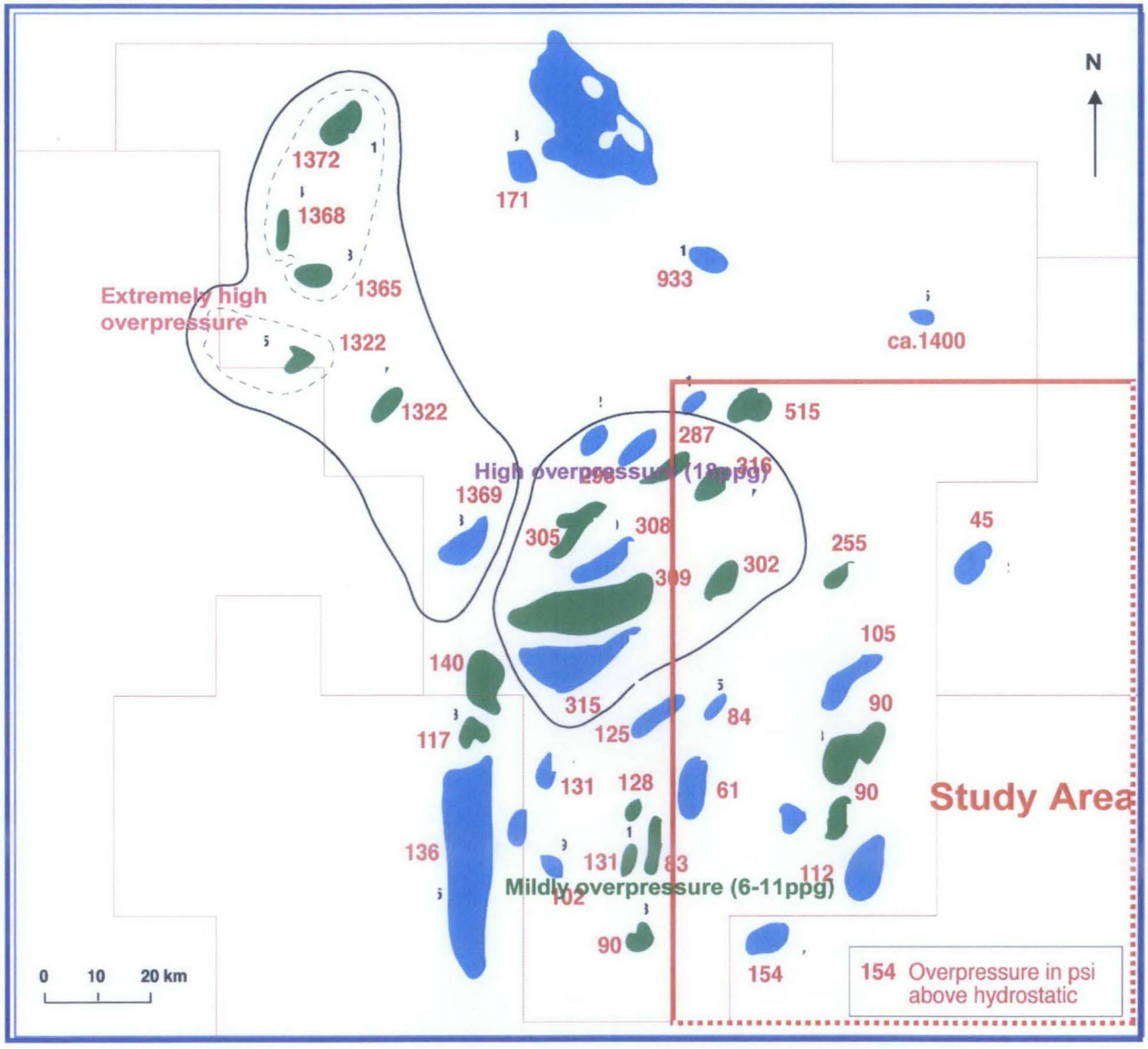

Fig. 2.6 Overpressure distribution in Central Luconia. The study area is in the red box which falls in the mildly overpressured area.

Chapter 3:
Phase 1: Pore Pressure Prediction in the Carbonate

3.1 Methodology

A combination of pre drill and post drill groups was applied in this study. In the post drill groups, the Predict Drillworks software was used to derive the normal compaction trend and pore pressure in each selected wells. The results are then correlated to the distribution of selected wells to see the regional pattern of the pressure regime in the study area. This study is done in the first phase of the study.

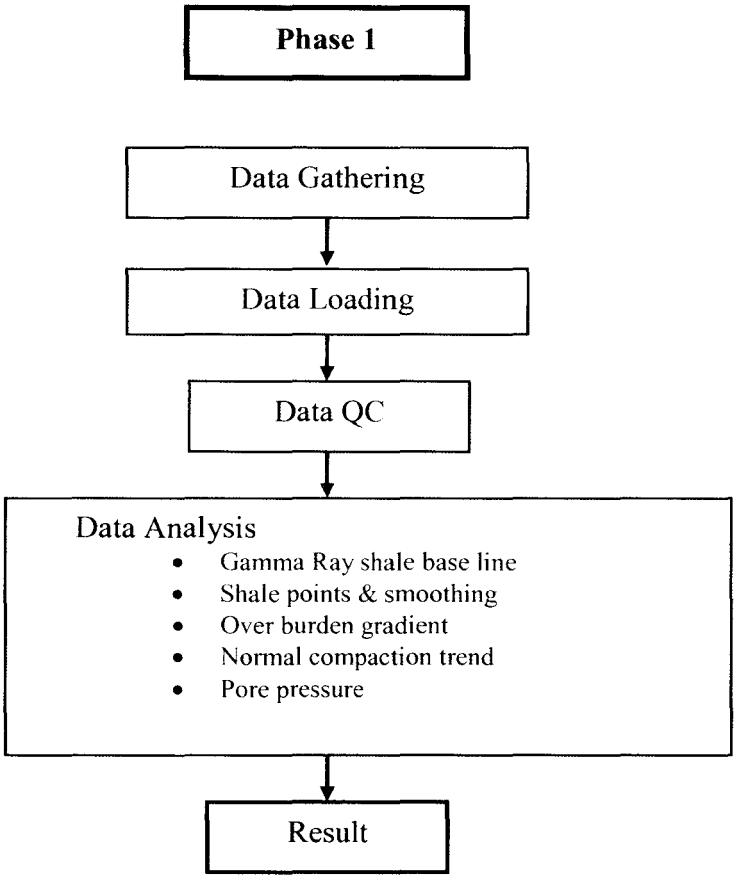

Fig. 3.1 Work flow for the first phase of the study.

3.2 Data Management

During the early stages, the arrangement of data needed is very crucial. The question of what type of data needed, where to get the data, how to access the data, how to extract the correct data, which to do first, which data has priority over the other, data confidentiality, the sensitivity of the study area have to be addressed. To solve the question effectively, a test run of the software using the tutorial dataset is necessary to know the data needed and the information required to enhance the understanding of the software itself. A base map consisting of fields, prospects and well locations also important to facilitate well data selection.

3.2.1 Data Handling

Firstly, a literature review was conducted to find out about the study area and the study itself. Reading material such as articles, journals, books and discussions with supervisors and technical staff of PETRONAS are the prime sources to access the information.

After determining the workflow, a base map was used to select wells that are located within the study area. Data needed for this study is then listed through a test run from the software (Fig. 3.2). The next step is how to get the data. There are various ways to get various data. Each way to access the data were listed and actions have been taken after that (Fig. 3.3). After obtaining the data, a list of the available data was made (Appendix A). From the list, wells are then selected to represent the study area.

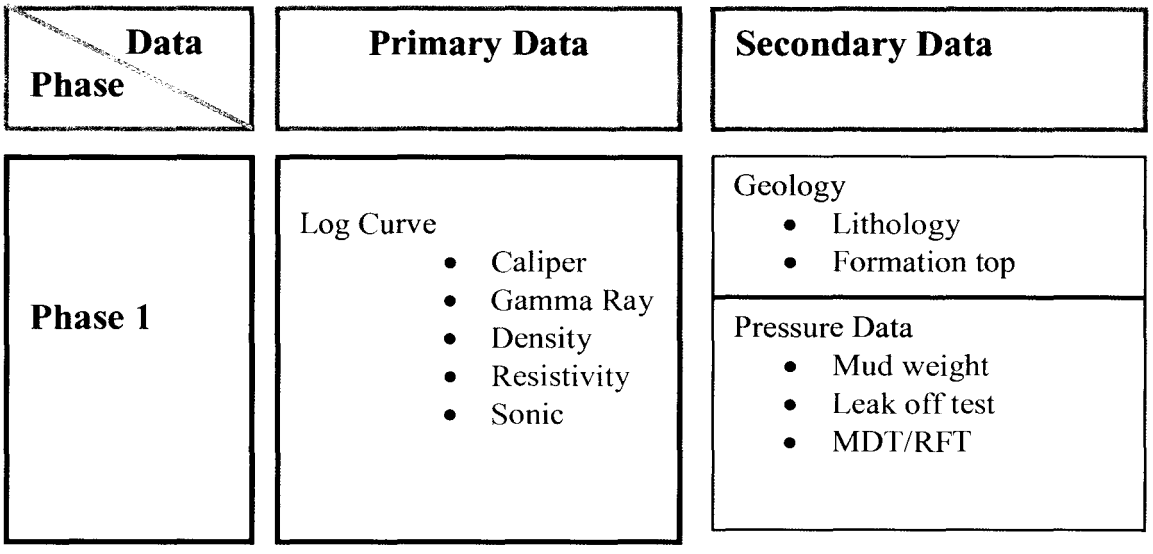

Fig. 3.2 Data needed to run the pressure analysis in the first phase.

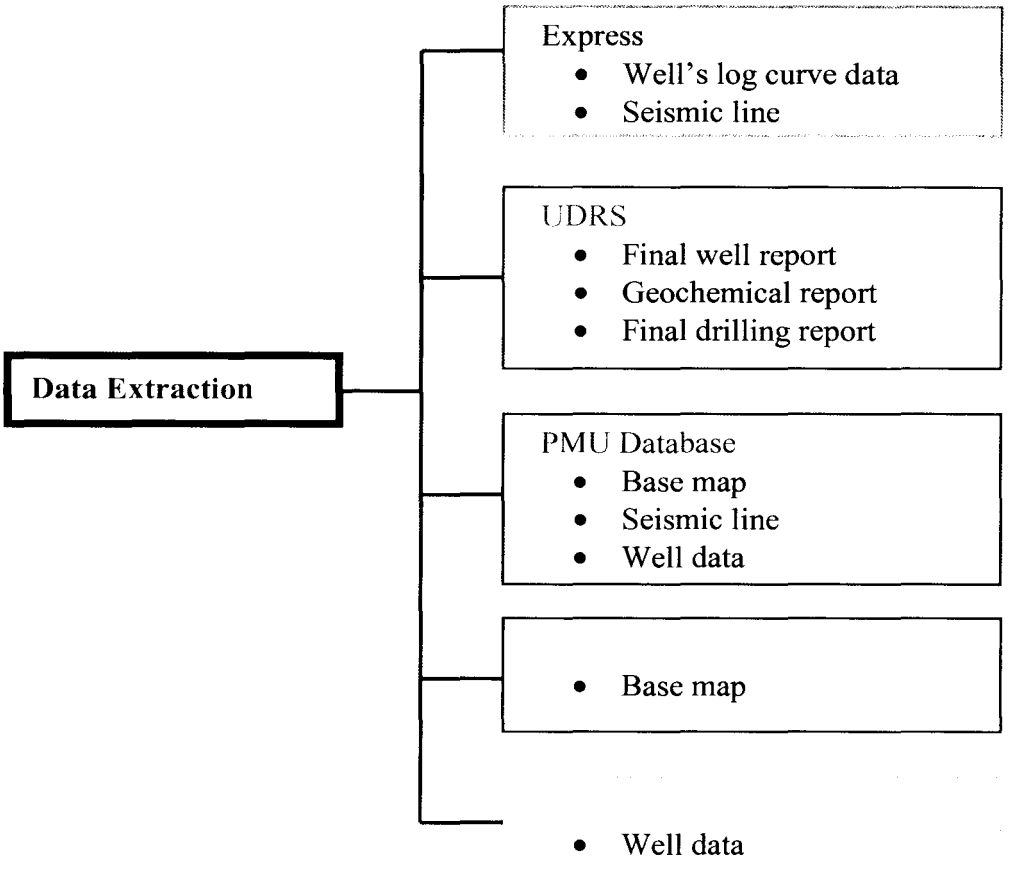

Fig. 3.3 Various ways to obtain the data required for the first phase of this study.

3.2.2 Data Loading

A project follows by a well were created in the Drillworks Predict software. Well data was then imported into the created well. ascii, las or lis data formats are the only formats that can be imported into the well data. Following this, a selection of wireline logs can be loaded; these comprise the Caliper, Gamma Ray, Resistivity and Sonic curves. The logs data must be arranged as per the saved format to allow data loading. Another approaches to data loading is by using the 'create a dataset' function key. This function allows the user to copy and paste the data needed into a form that the software can accept. After this step is completed, a view window is created by copying an empty default track. The loaded curves/datasets are then added to each track as per user creativity.

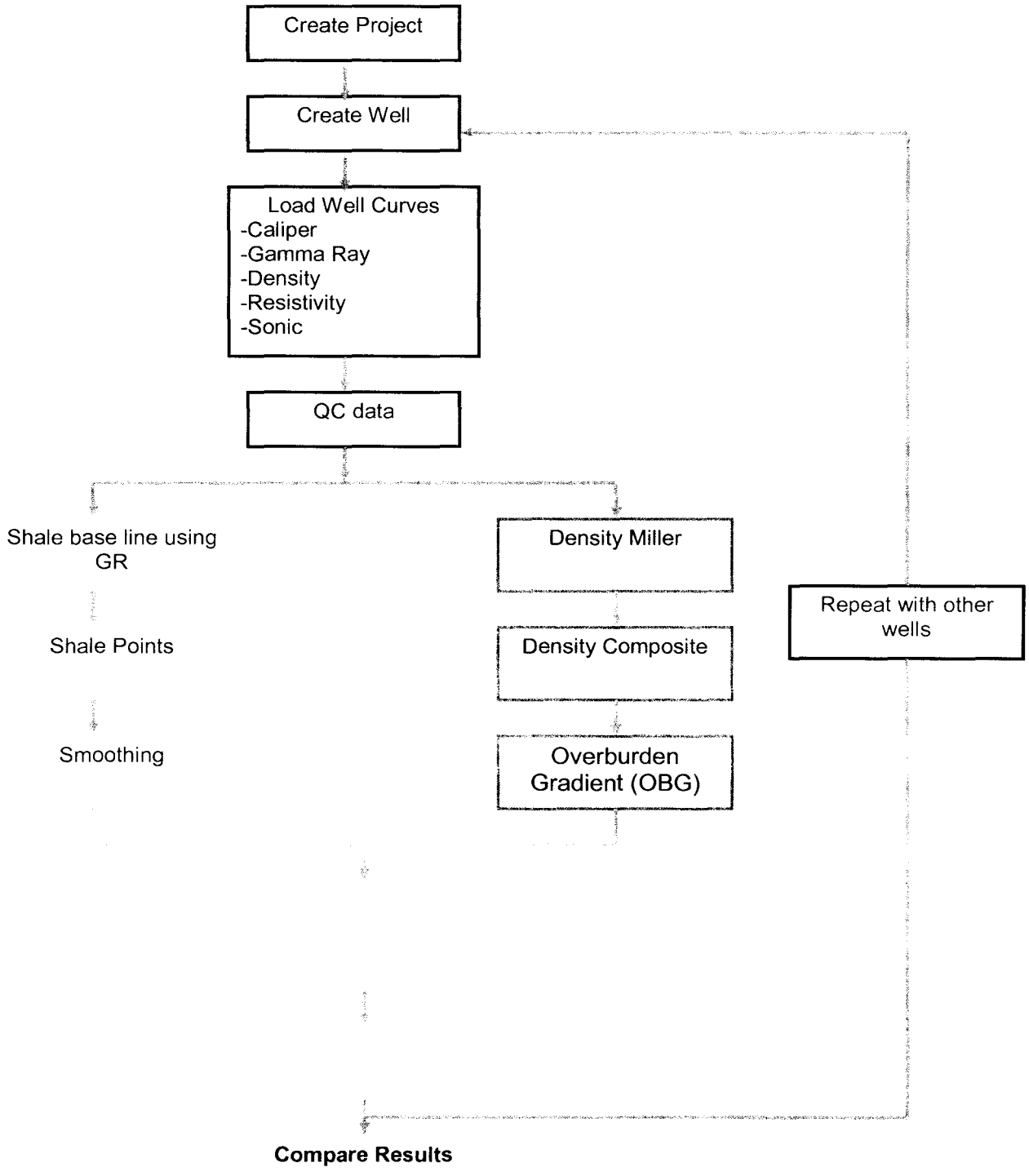

Fig. 3.4 The Drillworks Predict flowchart.

3.2.3 Data QC

The data were first screened using caliper log to remove those intervals that are affected by borehole condition. Bad borehole conditions such as caving will affect the readings, so the data need to be removed by calibrating it to the caliper reading. The other reason to screen the data is because of the existence of the spiking and the skipping effects. All these effects will impact on the analysis, resulting in unacceptable results. To avoid it, the bad data has to be removed from the dataset.

3.3 Data Analysis

In this study, a total of 10 wells were selected after screening the data availability from reports and database (Appendix A). These ten wells (A to J; Fig. 3.5) are well distributed across the study area. Schematic diagram showing the well penetration of the ten wells is shown in Fig. 3.6.

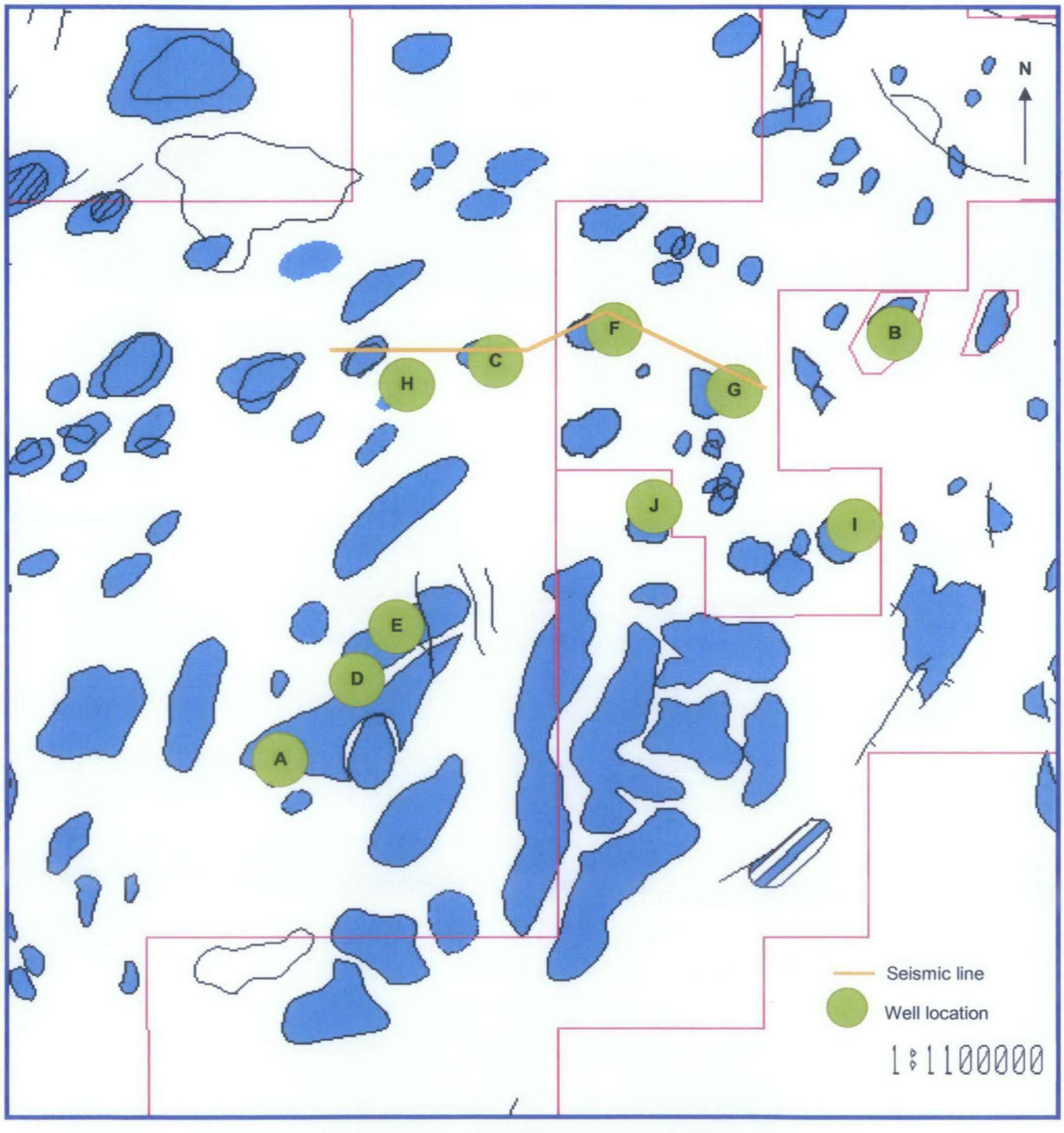

Fig 3.5 A location map showing the ten wells chosen to represent the study area. The orange line represents the seismic line used for the basin modeling.

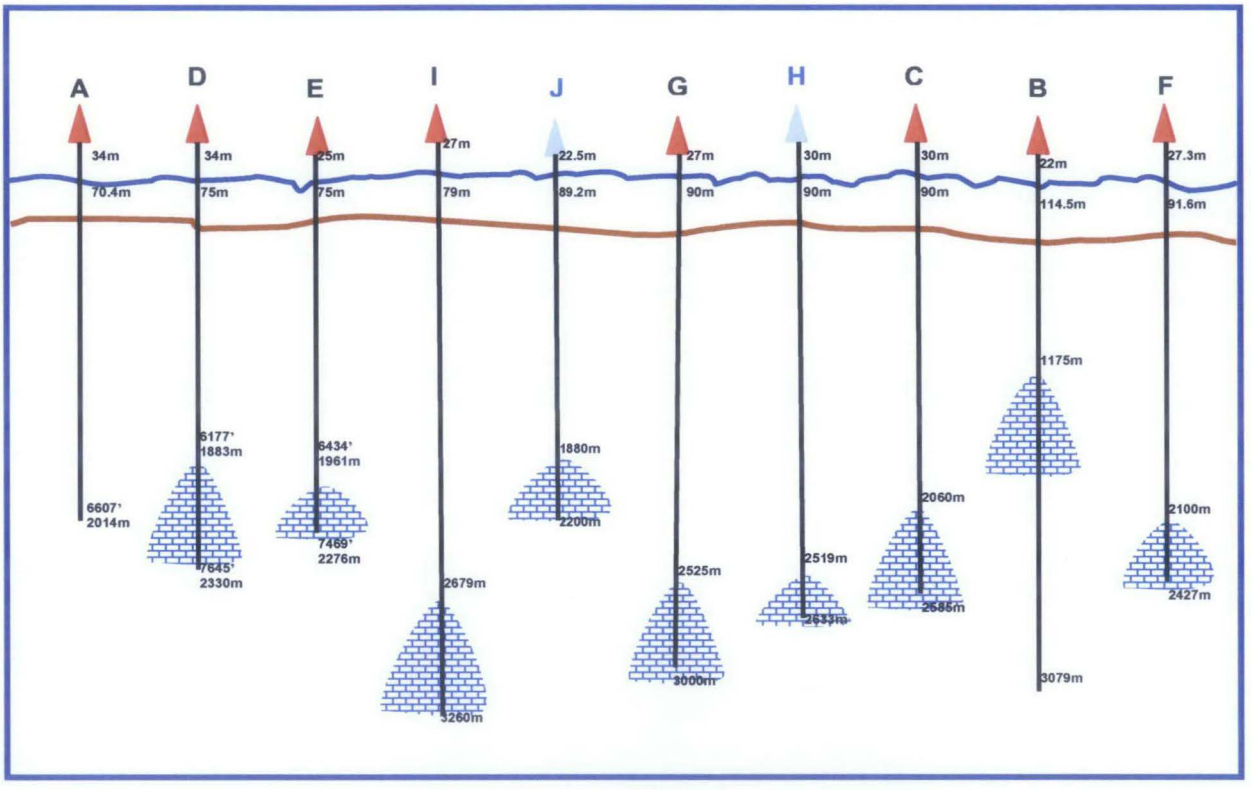

Fig. 3.6 The well penetration chart showing the height of the air gap, the water depth, the top of carbonate and the total depth. Gas discovery wells are marked in red, while dry wells are in blue.

3.3.1 Shale Lithology

After screening the dataset, the first thing to do in the analysis is to set a shale base line on gamma ray curve. A clean shale need to be selected in order to obtain good results. The selected shale intervals were cross checked with the lithology recorded in the mudlog section, well reports and composite logs. The shale base line was created by creating a line group based on the Gamma ray curve. The shale base line was drawn according to the clean shale package in the section.

Based on the Gamma Ray signature in the study area, the shale base line can be divided into three sections (Fig. 3.7). The obvious section is the boundary between the clastic and the carbonate because the gamma ray readings showed a marked shift. The 'carbonate shale section' referring to the existence of shale within the carbonate. This major shift is supported by the change of lithology shown in the mudlog and the reports. Besides the carbonate section, there are several sections occurring in the clastic group. The shift is also obvious but the reason for this shift in the clastic is unknown. After referring to the reports, it shows that the change of the clastic signature is because of the different of the stratigraphy and the time of deposition. Two shale sections, called the 'top shale section' and 'middle shale section' were delineated based on the regional signature of the Gamma Ray curves in all the 10 wells.

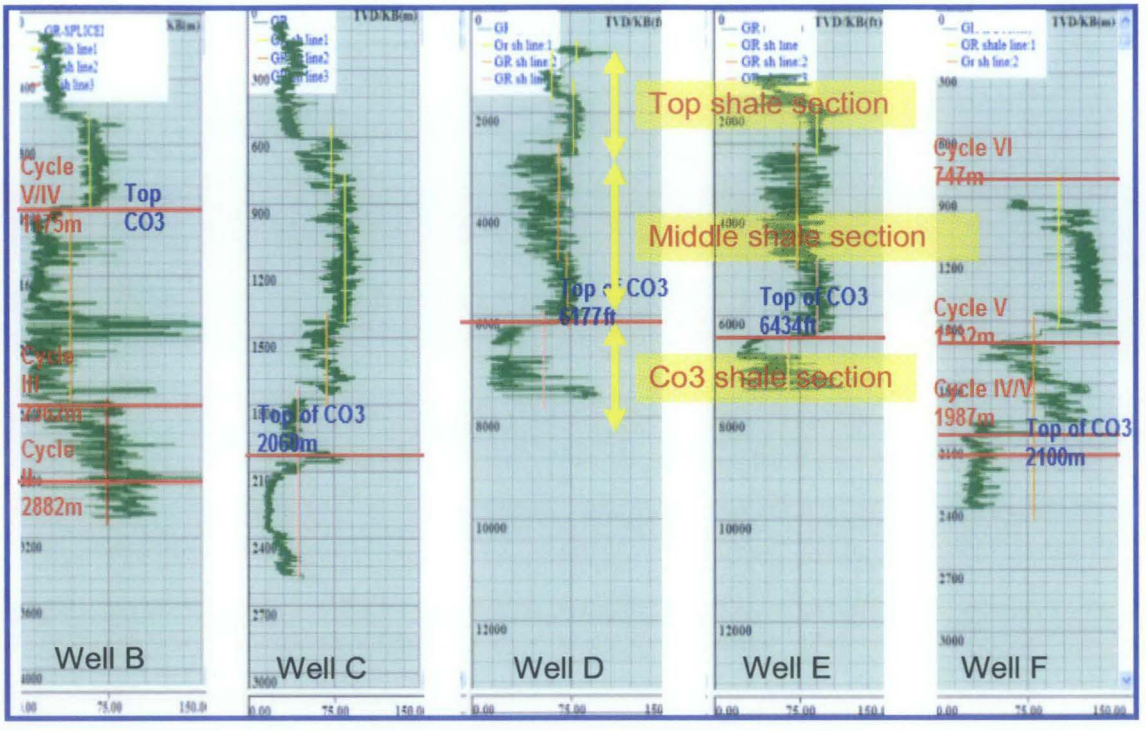

Fig. 3.7 Examples of gamma ray segmentations indicating the changes in lithology, stratigraphy and time of deposition.

3.3.2 Shale points and smoothing

Shale points were created based on gamma ray as the lithology dataset, gamma ray shale base line as the line group and a porosity data type for sonic and resistivity curve. Each shale point generated (from resistivity or sonic curve) need to be smoothed using moving weighted average (MWA) method. This step was done to get the average value of the curve based on the shale line generated. The smoothing of the curves helps reduce the data scattering, allowing easy picking of the normal compaction trend (NCT). Both shale points and smoothing were conducted on the resistivity and sonic curves.

For smoothing, a few values were used as the number of filter points, and finally the chosen value is 51. A comparison of the number of filter points of 3, 15, 51, 101, and 501 is illustrated in Fig. 3.8.

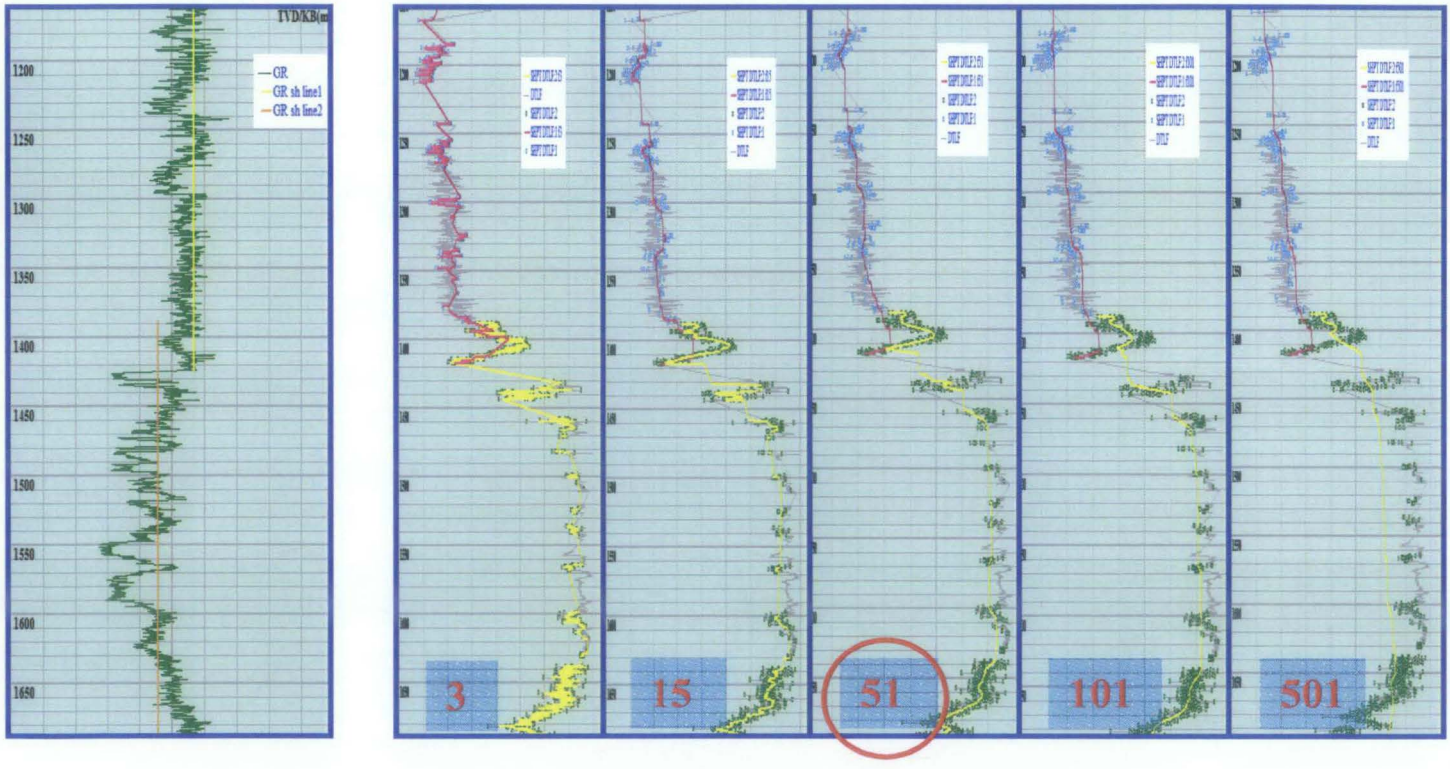

Fig. 3.8 A comparison of number of filter points of 3, 15, 51, 101, and 501 compared to Gamma Ray and Shale base line. The red circle indicates the number filter points chosen.

3.3.3 Over Burden Gradient

Overburden gradient (OBG) analysis was done using the density curve. The density curve is commonly only measured in the middle of the well to the bottom hole i.e. in the zone of interest. Thus, the density curve need to be calculated and simulated for the upper part of the well. Using Miller's equation, the density at the top part of the well is calculated. By using the existing density curve and Miller's density, a composite of density is created. Finally, the OBG or lithostatic line was calculated using the composite density.

A composition of the OBG of the 10 studied wells in the area is shown in Fig. 3.9. A similar trend was observed in all the nine wells, with the exception of well B. The Well B OBG line is tilted at depth about 1400m. This trend shows that Well B well has a slight different trend from the rest of the wells, indicating that Well B has a slight low overburden in the area and has a slight over pressure at the greater depth section. This hypothesis will be further studied with the Normal Compaction Trend (NCT) in the next step.

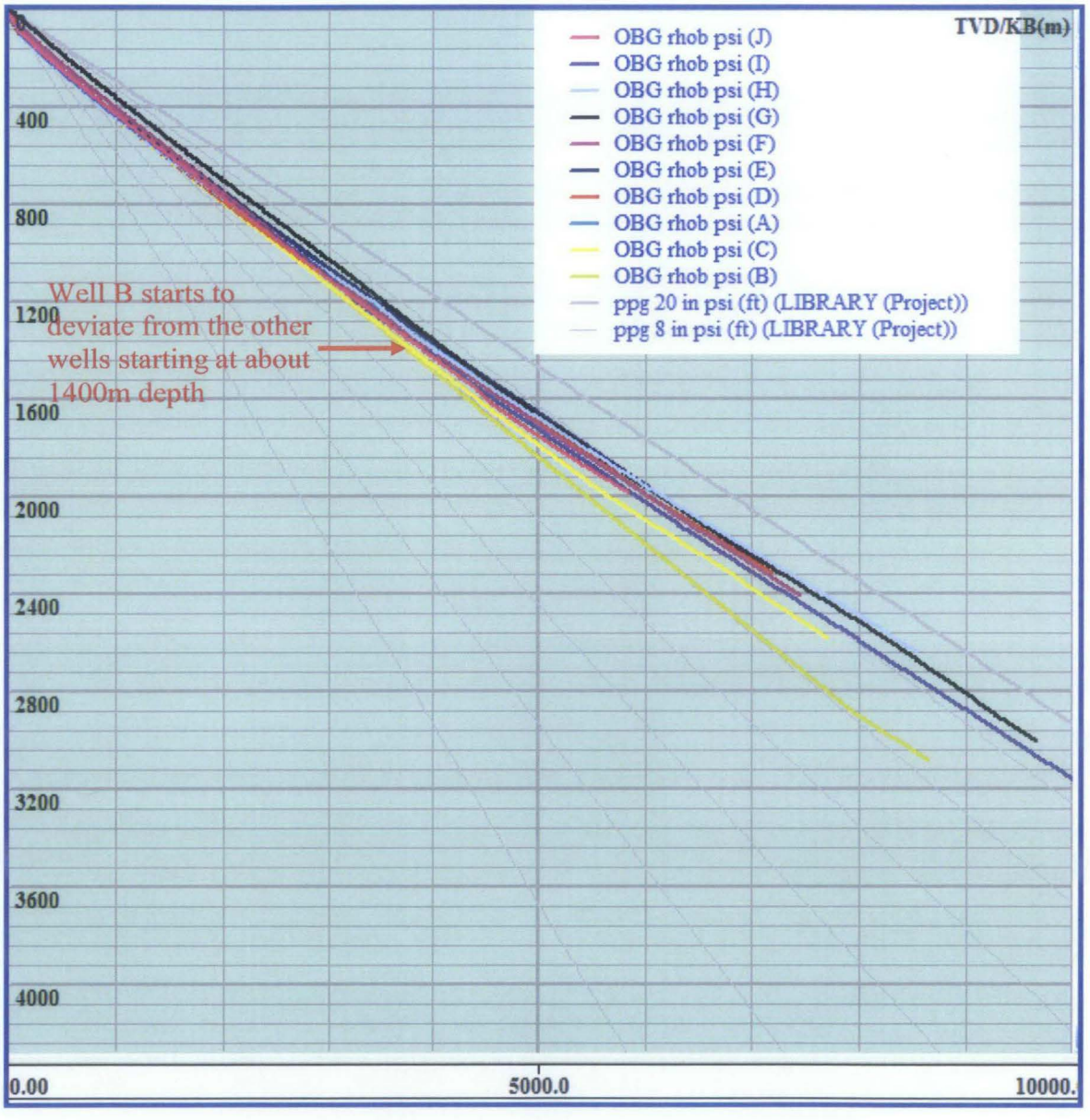

Fig. 3.9 Compilation of the overburden gradient (OBG) in the studied wells.

3.3.4 Pressure Data

Pressure data is needed to calibrate the results and the formation pressures are measured while drilling. The pressure data are obtained from mud weight, leak off test and MDT/RFT where available. These measurements were placed in one track with the calculated OBG in the previous steps. In this track also, various lines of pressure ranging from 8ppg to 20ppg is placed to make it easier to read the pressure measurement. For standardization purposes, all the measurements were converted into pressure per square inch (psi). This pressure data track was prepared to place the pore pressure prediction in the next steps. The pressure prediction calculated from the different methods will be placed in this track so that the accuracy can be monitored. All the pressure data and the pore pressure should not exceed the OBG/Lithostatic line. The exceeding data should be checked because there must be an error of extracting the data during the calculation.

3.3.5 Normal Compaction Trend (NCT)

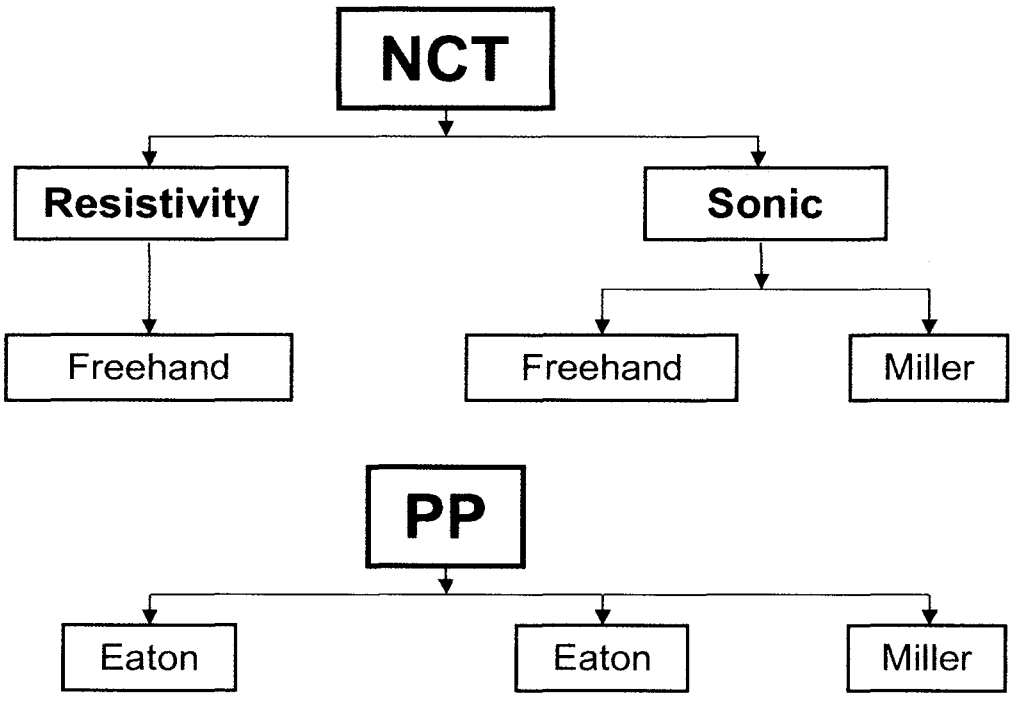

Fig 3.10 The Normal Compaction Trend and Pore Pressure calculation workflow.

The Normal Compaction Trend (NCT) is a very crucial step in order to determine the Pore Pressure (PP). There are several equations that can be used to calculate the Pore Pressure. The widely used traditional methods are the Eaton's and the Miller's methods. In this study, three methods were employed, using two different equations from Eaton and Miller (Fig. 3.10). The three methods are the Pore Pressure Miller's equation using NCT calculated from the Miller's equation, the second method are the Eaton's Pore Pressure equation using the visualized freehand drawn NCT on the resistivity curve, and the third method is the Pore Pressure calculation using the visualized freehand drawn NCT using the Sonic curve. These three methods will be elaborated in the Pore Pressure section. In this section, the NCT will be divided into two methods that is the Miller's and the visualized freehanddrawn methods.

3.3.5.1 Miller's Method

Miller's sonic equation for normal compaction trend is expressed as below,

$$DT_{norm} = \frac{DT_{ml}}{\frac{DT_{ml}}{DT_{matrix}} + \left[1 - \frac{DT_{ml}}{DT_{matrix}}\right] \exp(-\lambda \sigma_{norm})}$$

Where

DT = sonic travel time

DT_{ml} = sonic travel time at mudline (200ft/sec)

DT_{matrix} = sonic travel time of matrix material (14000 ft/sec – 17000ft/sec for "shales")

σ_{norm} = effective stress assuming normal pressures is an empirical value that yields the best fit for the relation between velocity and effective stress at the location of interest.

In Miller's method, the λ parameter was varied to get the best fit with the smoothed shale points. Different λ values were observed in all the wells. The pattern shows that λ in the top shale section always has a higher value than the λ in the middle shale section. However in Wells B and I, this observation was reserved. The difference in Well B is quite high, while in Well I, there is just a slight difference (Table 3.1). If we compare this result to the OBG, we can see that Well B most probably have an overpressured zone in its deeper section.

The results of the Normal Compaction Trend (NCT) in all the ten wells studied shows that there are 4 groups in the top shale section (Fig. 3.11) and a total of 3 groups in the middle shale section (Fig. 3.12).

In the top shale section, the divisions are: Well I and Well B are in the first group, Well D, Well H, and Well E in the second group, Well J, Well F, and Well C are in the third group, while Well A and Well G are in the fourth group. The first has the highest rate of compaction compared to the other groups, and the other groups follow with descending rates of compaction.

In the middle shale section, the divisions are: Well E and Well C are in the first group, Well A, Well D, Well I, and Well J are in the second group, while Well H and Well G is in the third group. As was observed in the top shale section, the first group has the highest rate of compaction compared to the other group and the other groups follow with descending rates of compaction. In this middle shale section, Well B is out of the three groups. It has the lowest compaction rate indicating that the sediments were not normally compacted or under compacted. The under compacted scenario can be relate to the overpressure regime where sediment cannot be compacted due to the existence of the pressure holding the vertical loading from the sediment infill.

NCT	Parameters	Well A	Well B	Well C	Well D	Well E	Well F	Well G	Well H	Well I	Well J
Miller 1	Normal PPG (kPa/m)	10.28	10.28	10.28	10.28	10.28	10.28	10.28	10.28	10.28	10.28
	Mudline sonic (us/m)	656	656	656	656	656	656	656	656	656	656
	Matrix sonic (us/m)	230	230	230	230	230	230	230	230	230	230
	Lambda	0.00015	**0.0004**	0.0002	0.00025	0.00022	0.00018	0.00015	0.00023	**0.0004**	0.0002
Miller 2	Normal PPG (kPa/m)	10.28	10.28	10.28	10.28	10.28	10.28	10.28	10.28	10.28	10.28
	Mudline sonic (us/m)	656	656	656	656	656	656	656	656	656	656
	Matrix sonic (us/m)	230	230	230	230	230	230	230	230	230	230
	Lambda	0.00035	**0.0002**	0.0004	0.00035	0.0004	0.0003	0.00027	0.00027	**0.00035**	0.00035

Table 3.1 Different Lambda value used in the Miller calculation in the constuction of Normal Compaction Trend.

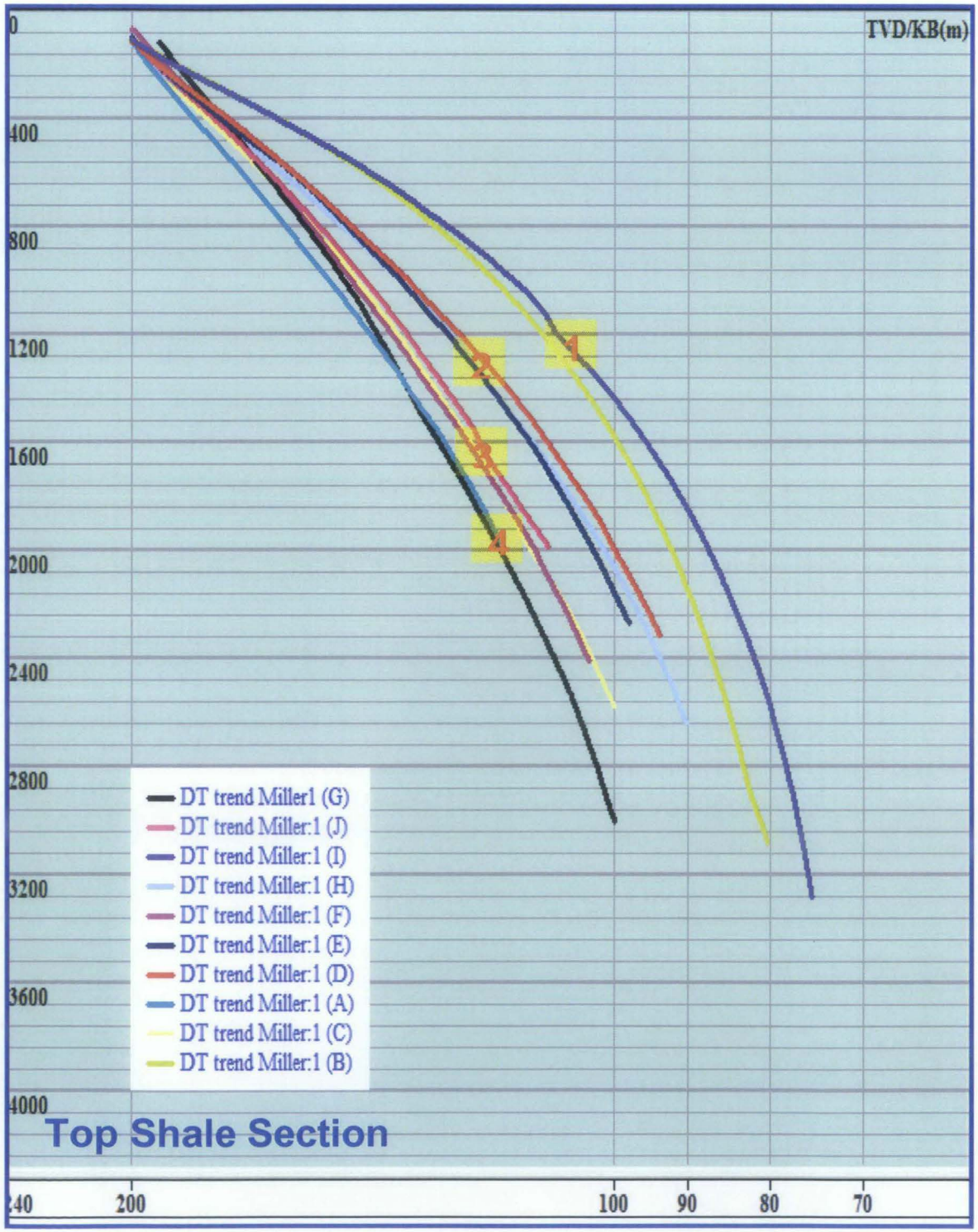

Fig. 3.11 The NCT of the top shale section Miller's equation on sonic curve.

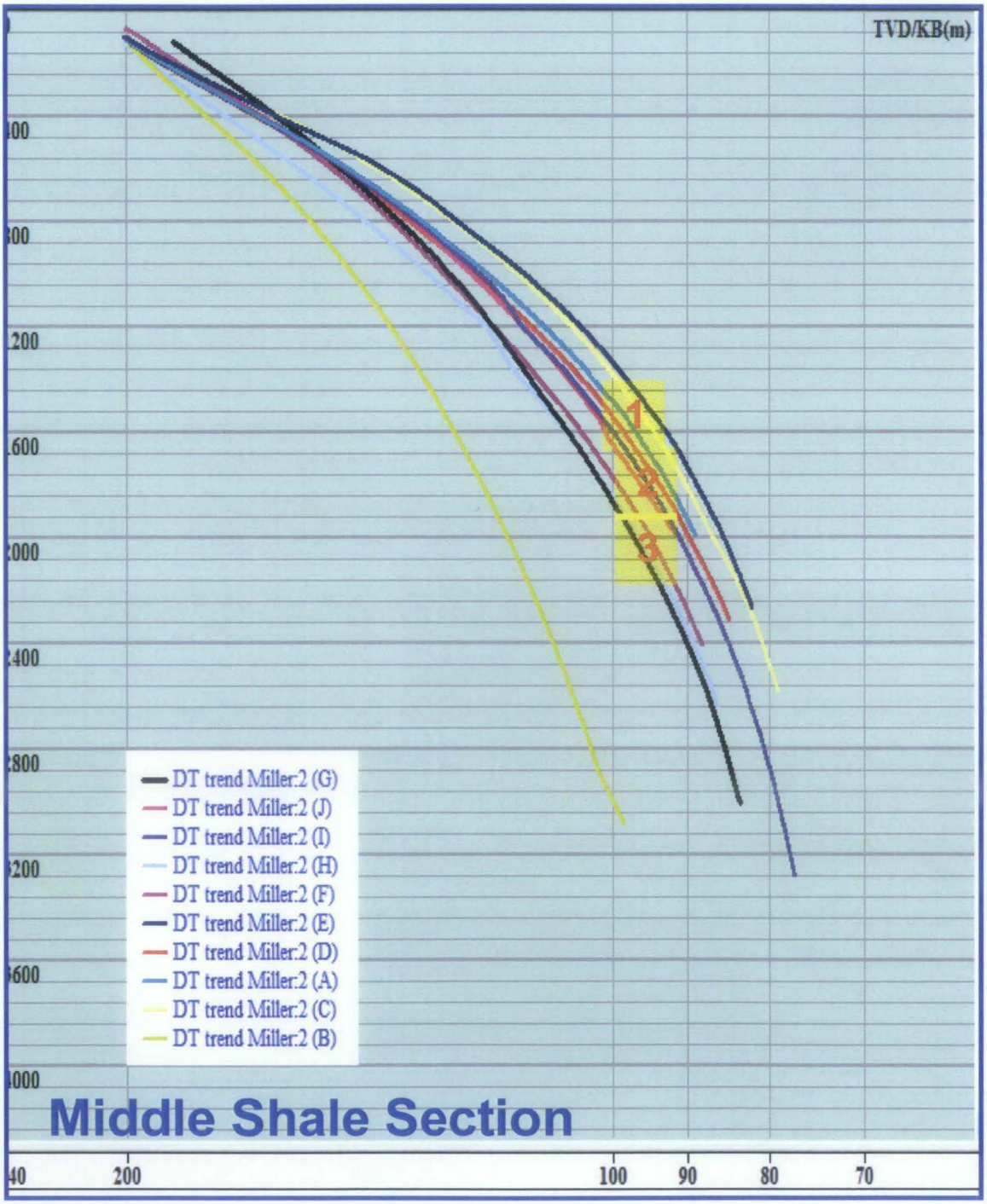

Fig. 3.12 The NCT of the middle shale section using Miller's equation on sonic curve.

3.2.5.2 Visualized Freehand Drawn NCT for Eaton's Pore Pressure Method

The second way to determine NCT was visualized freehand drawn method. The freehand drawn NCT is based on the smoothed curves. This freehand drawn NCT is for the Pore Pressure analysis using Eaton method. The freehand drawn NCT was drawn on two different curves, that is the resistivity curve and the sonic curve. The freehanddrawn NCT in resistivity curve can be observed in Fig. 3.13 and Fig. 3.14 and freehanddrawn NCT in sonic curve are shown in Fig 3.15and Fig. 3.16. Each curve was divided into two sections, the top shale section and the middle shale section.

In all the three methods, there is large variation in the top shale section compared to the middle shale section. It is likely that the top shale section has a greater facies distribution relative to the middle shale section.

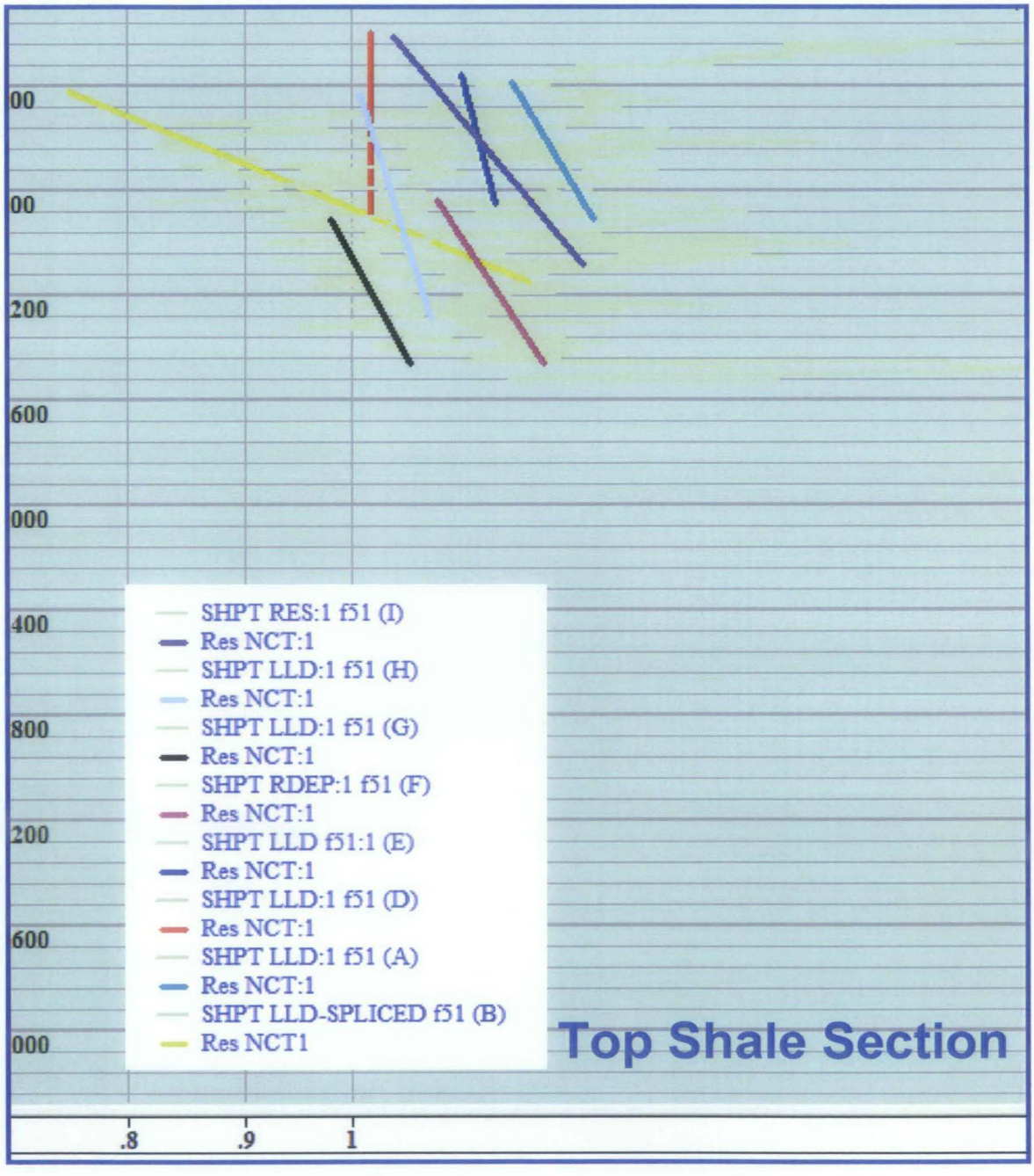

Fig. 3.13 The hand drew NCT for top shale section in the resistivity curve.

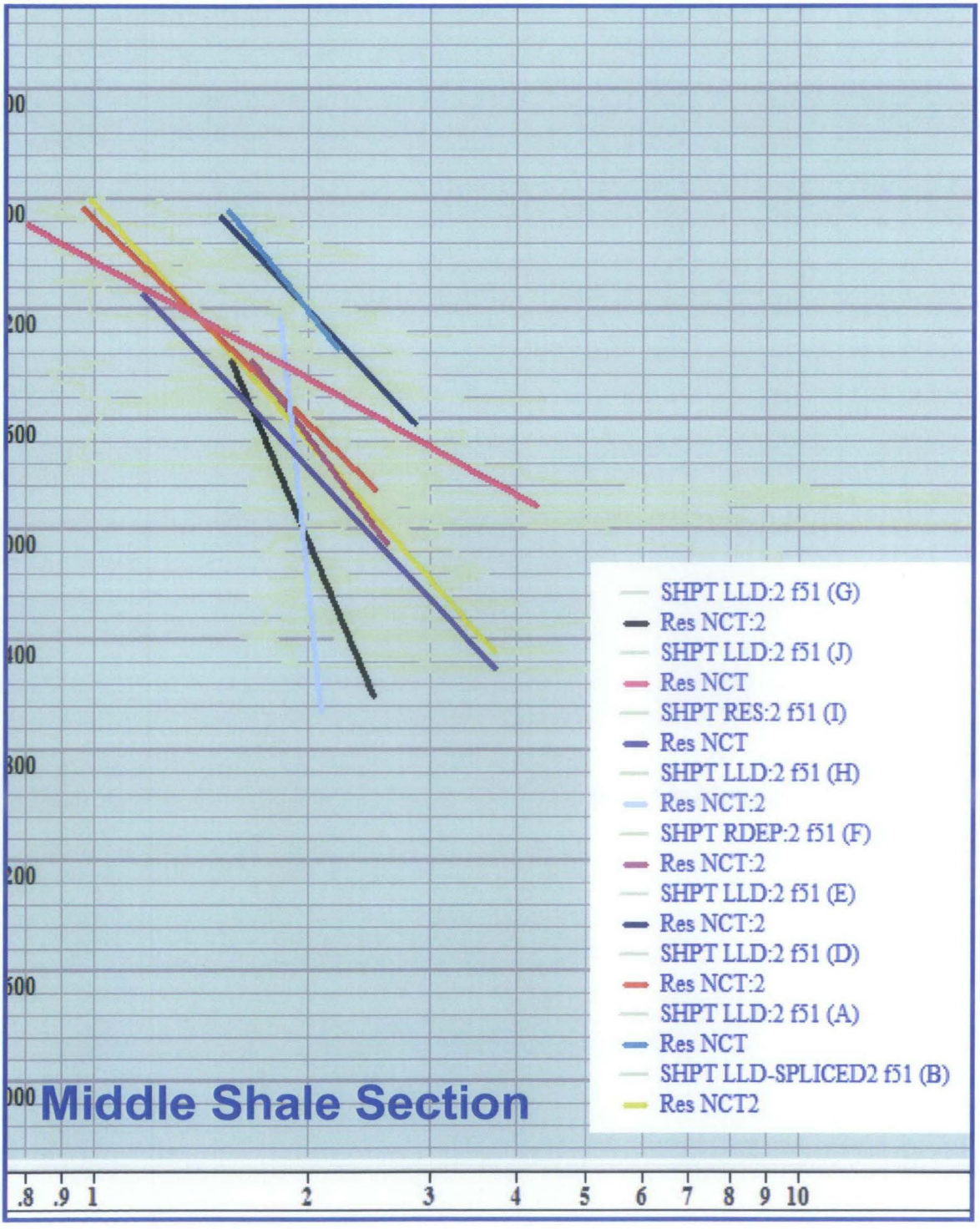

Fig. 3.14 The hand drew NCT for middle shale section in the resistivity curve.

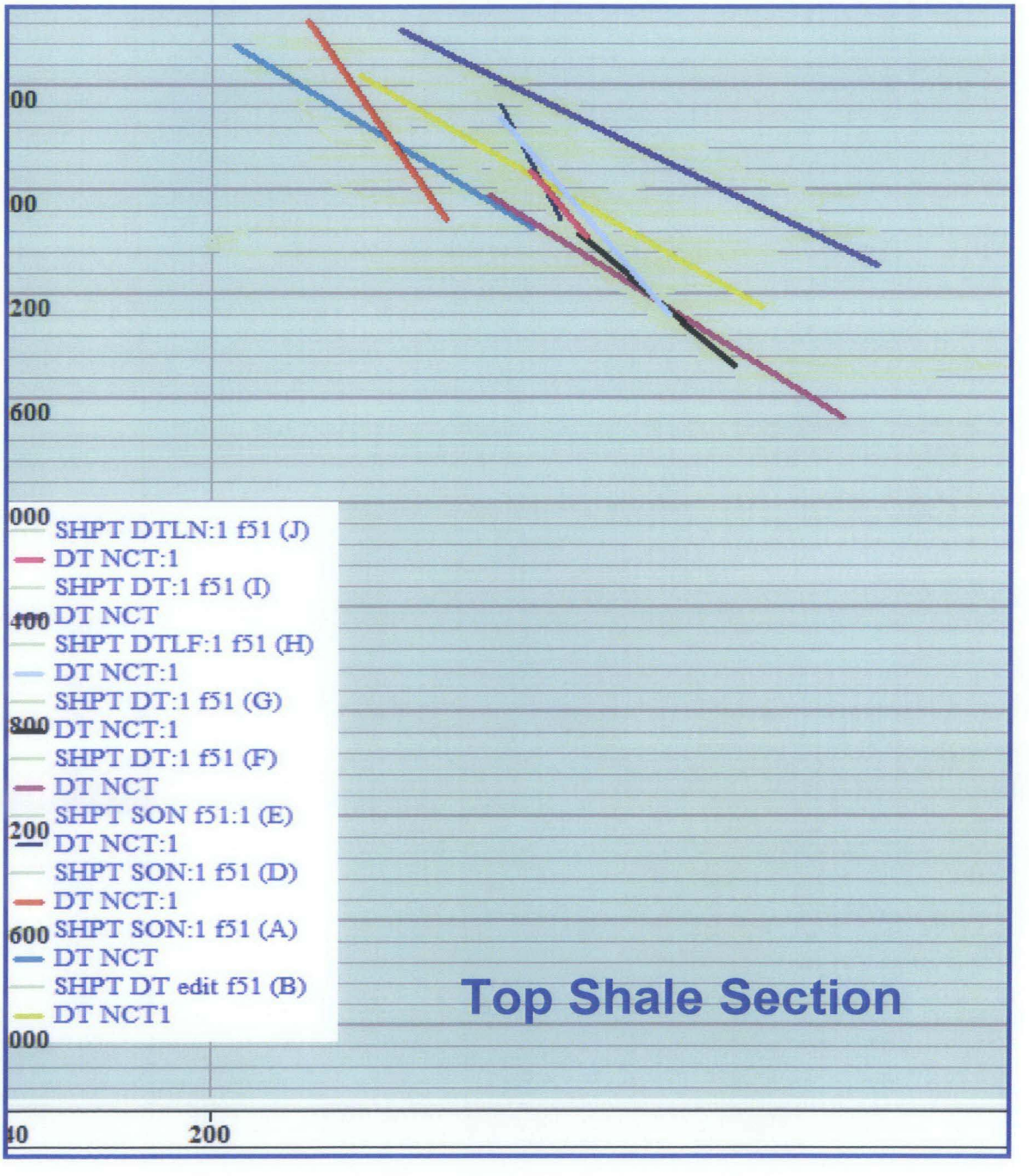

Fig. 3.15 The hand drew NCT for top shale section in the sonic curve.

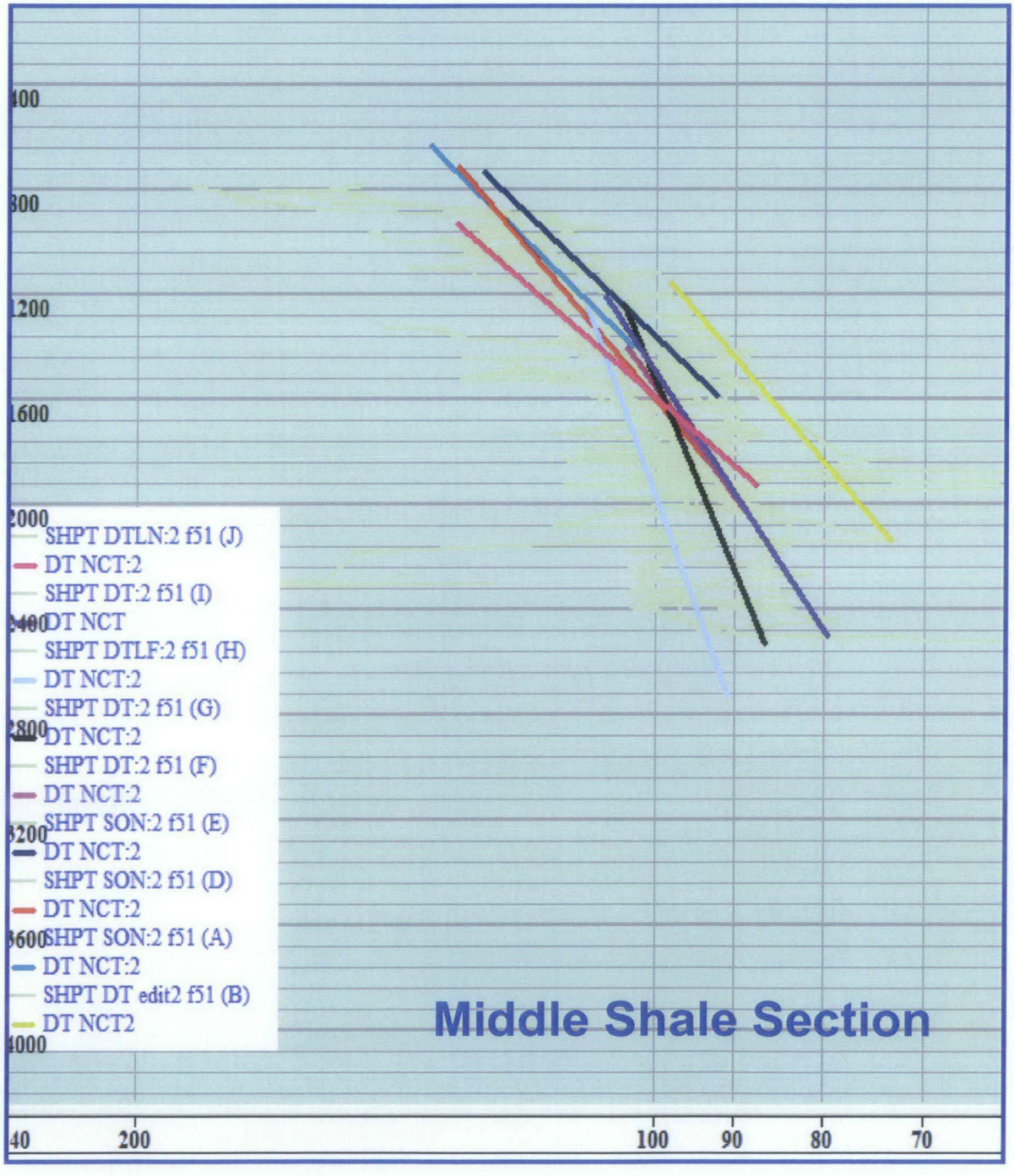

Fig. 3.16 The hand drew NCT for middle shale section in the sonic curve.

3.3.6 Pore Pressure Prediction

As stated in Normal Compaction Trend topic, there are three methods chosen to run the Pore Pressure prediction. The first is the Pore Pressure Miller's equation using NCT calculated from the Miller's equation (Fig 3.17), the second method is the Eaton's Pore Pressure equation using the visualized freehand drawn NCT on resistivity curve (Fig. 3.18) and the third method is the Eaton's Pore Pressure calculation using the visualized freehand drawn NCT using the sonic curve (Fig. 3.19).

In Miller's method, the equation can be expressed in both velocity and effective stress. In both equations, the λ parameter is very crucial as it impacts on the resulting NCT.

Miller's velocity equation:

$$V = V_{ml} + (V_{matrix} - V_{ml})\,(1 - e^{-\lambda \sigma e})$$

Miller's equation expressed in terms of effective stress

$$\sigma_e = \frac{1}{\lambda} \ln \left[\frac{V - V_{ml}}{V_{matrix} - V_{ml}} \right]$$

Modifying this equation allows the deviation of pore pressure, as shown below.

$$Pf = OBG - \frac{\frac{1}{\lambda} \ln \frac{V - V_{ml}}{V_{matrix} - V_{ml}}}{Depth}$$

Where σ_e = Effective stress

λ = Empirical fitting parameter which defines how velocity increases with increasing effective stress

P_f = Formation pressure

OBG = Overburden gradient

V_{matrix} = Interval velocity in the rock matrix

V_{ml} = Interval velocity in water (at the mudline)

Depth = Depth of interest

This is Miller's velocity/effective stress equation expressed in terms of pore pressure for the virgin compaction case.

Results from the first method were not very convincing as the calculated pore pressure mostly fell into the underpressure zone. As such, this method is not recommended for this study area.

The second and third methods were calculated using the Eaton's equation. In Eaton's method, the assumption is that the pore pressure is equal to the vertical stress minus the effective stress. With the assumption, Eaton's came out with a general form of the equation to calculate the pore pressure. In Eaton's equation, constant values for each resistivity and sonic wire line log curves for the x values (equation a and b). The x values are 1.2 and 3 for the resistivity curve and sonic curve, respectively.

Assuming that: $P_f = S_v - \sigma_e$

General form: $\sigma_e = \sigma_n (M_o/M_n)^x$

Resistivity: $\sigma_e = \sigma_n (R_o/R_n)^{1.2}$ .....equation (a)

Sonic: $\sigma_e = \sigma_n (\Delta t_n/\Delta t_o)^3$ .....equation (b)

Where P_f = Pore pressure

S_v = Overburden stress

M_n = Normal trend value for M

σ_e = Effective stress (vertical)

σ_n = Effective stress for normal pressure at current depth

M_o = Observed value for M

For the second method, the results seem to fit with the mud weight and repeat formation tester (RFT) readings but corrections for the resistivity logs were not done. The resistivity tool is sensitive to the temperature effect, hence a correction need to be carried out before it can be used for any analysis. So, the second method was also not applicable in this study.

Encouragingly, however, results from the third method fits quite well with the Repeat Formation Tester (RFT) readings. Therefore, this method was chosen for the analysis on predicting the pore pressure in the shale within the carbonate.

The comparison of pore pressure results using the three methods is shown in the Fig. 3.20.

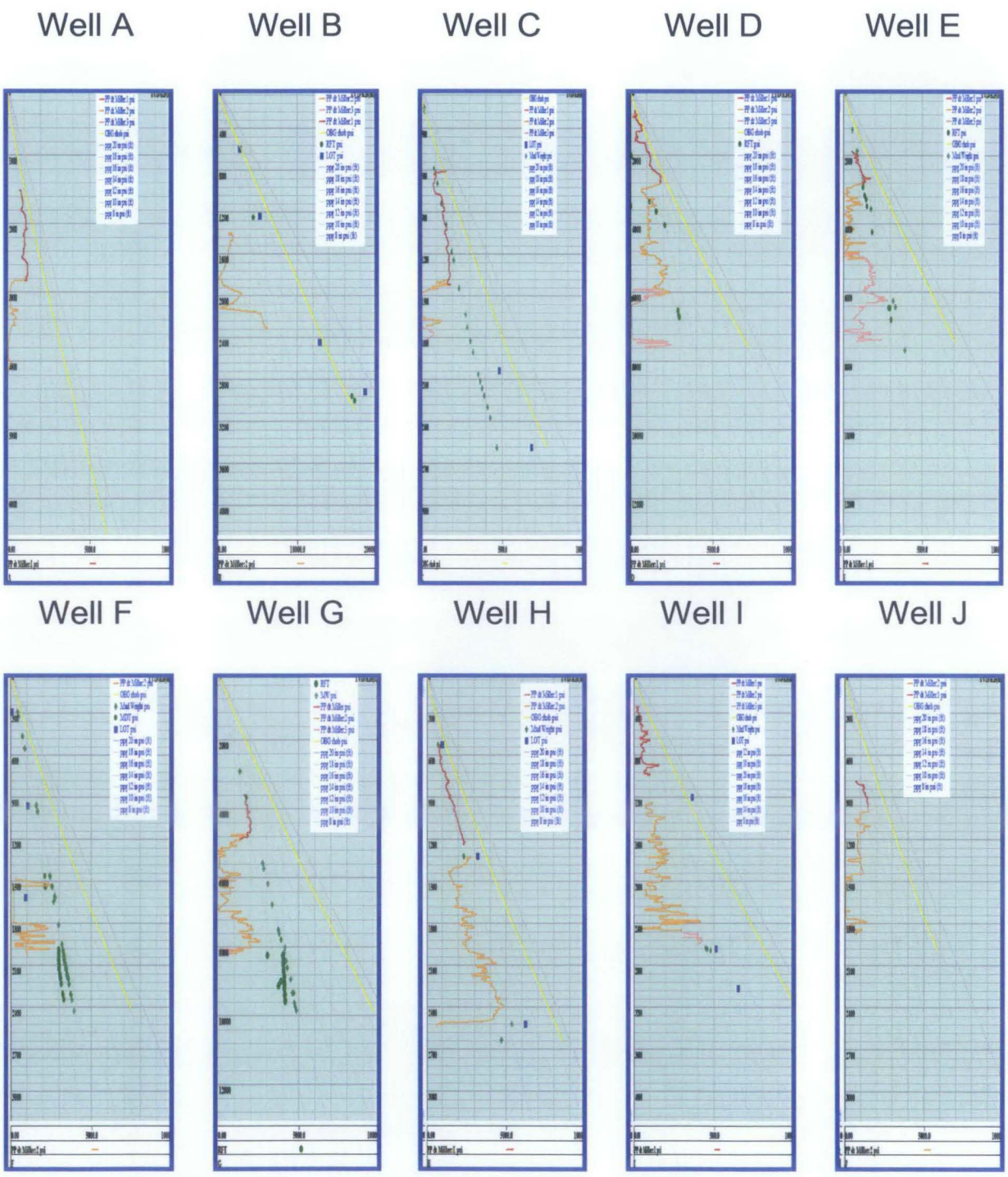

Fig. 3.17 The Pore Pressure Prediction using the Miller's equation on sonic curve.

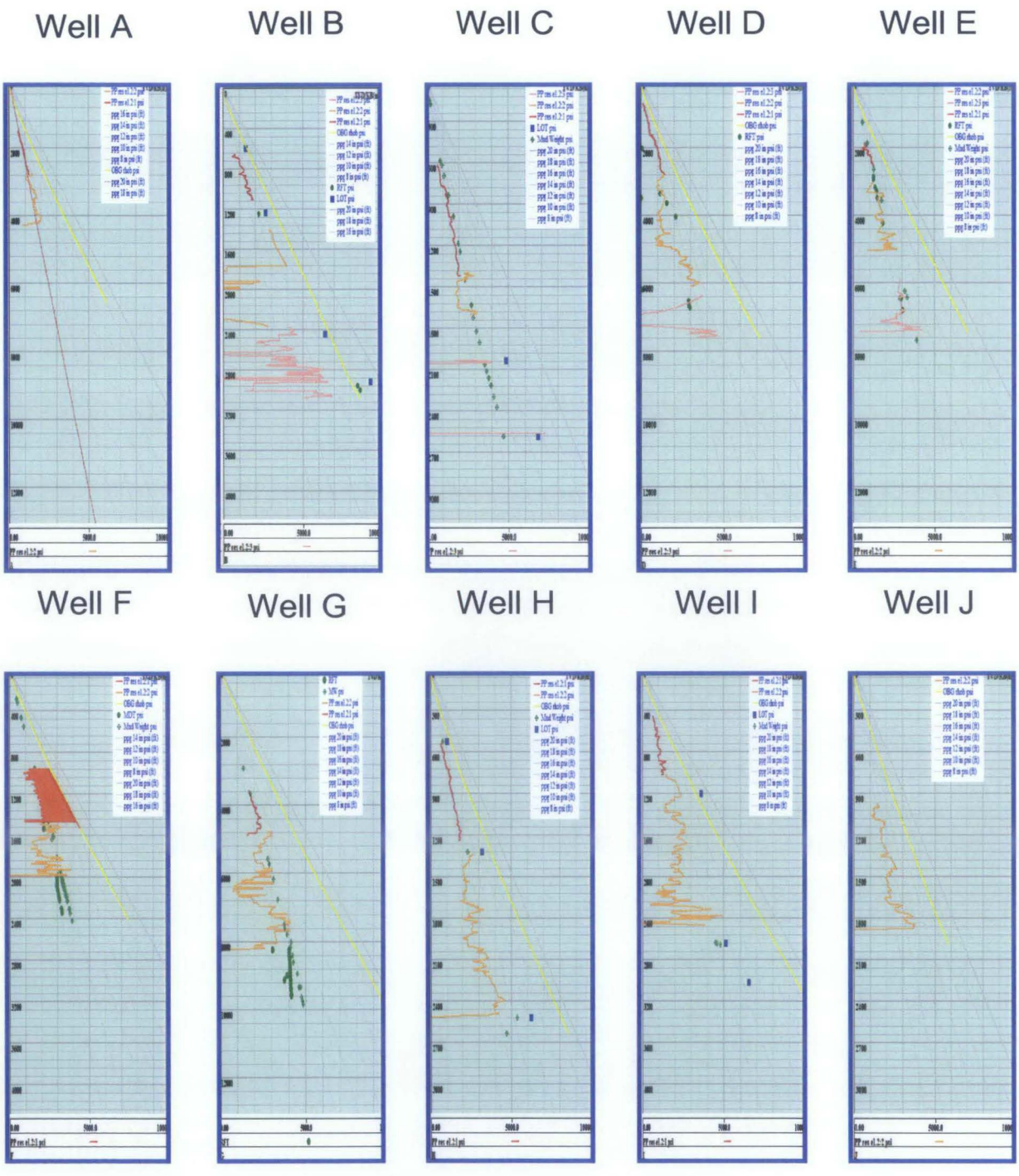

Fig 3.18 The Pore Pressure prediction using Eaton's equation on resistivity curve.

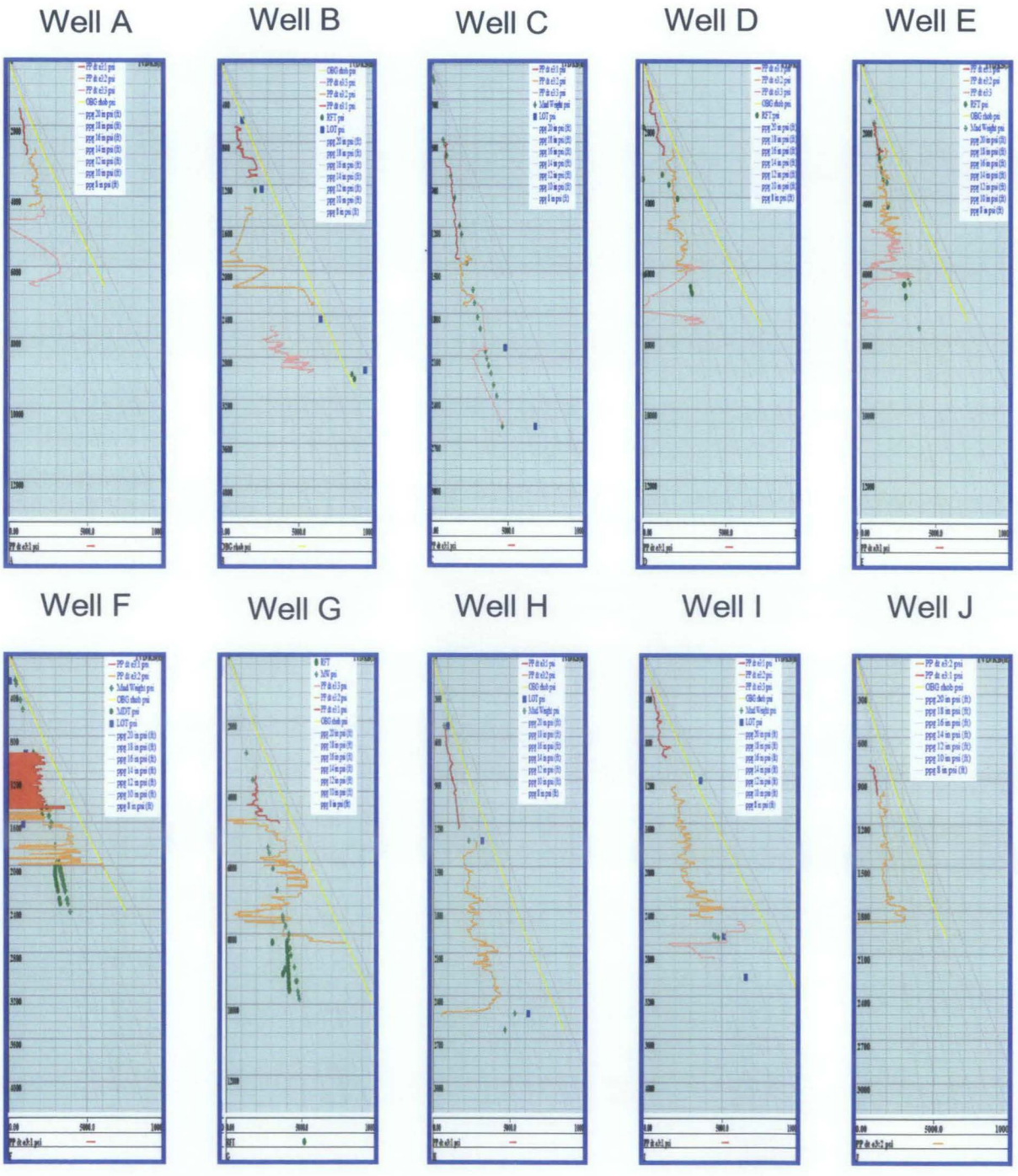

Fig 3.19 The Pore Pressure prediction using the Eaton's equation on sonic curve.

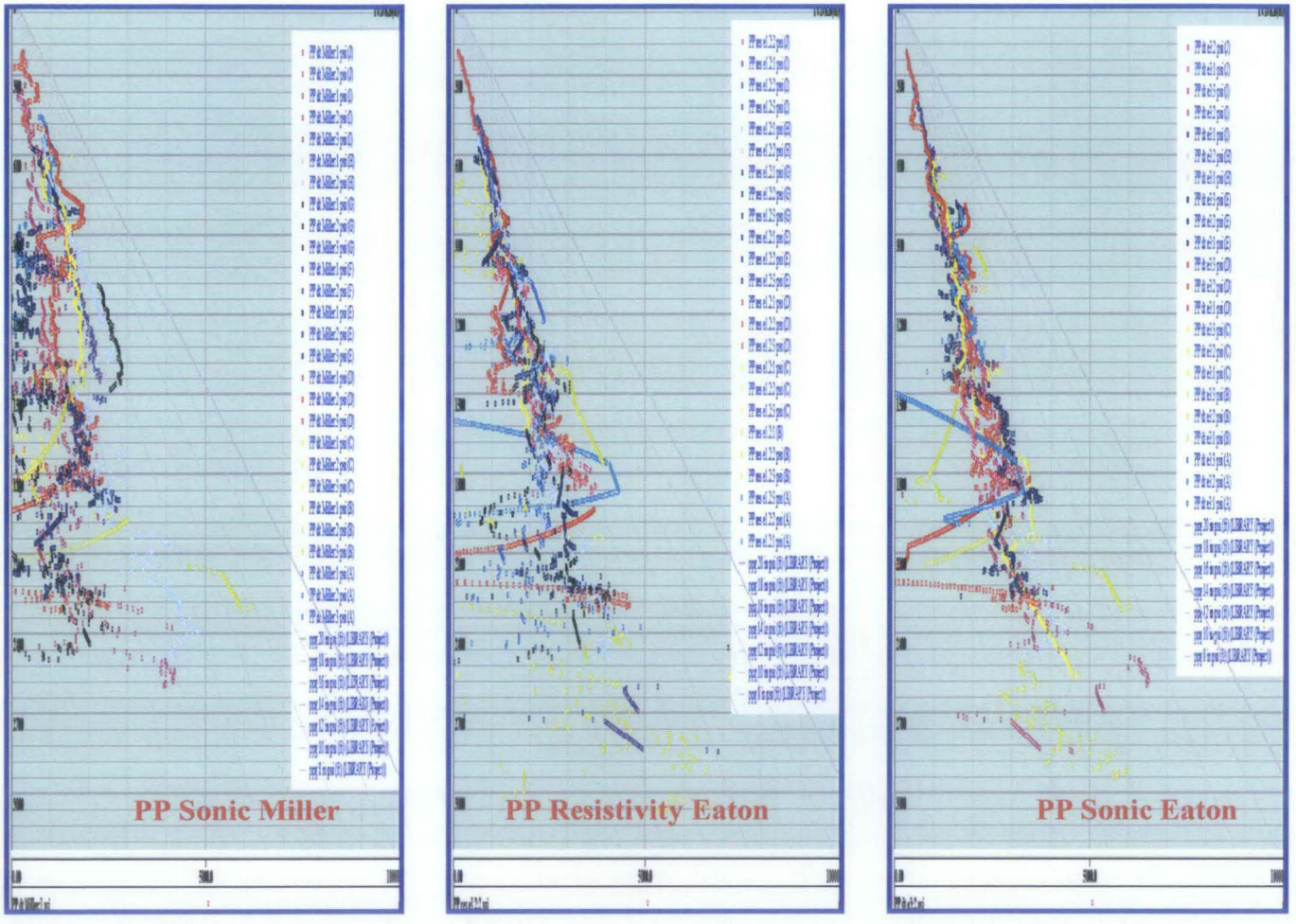

Fig. 3.20 The comparison of the three methods. The first method seems to falls in the under pressure zone, the second method was not corrected and the third method is the chosen method to run the analysis of prediction the pore pressure in the carbonate section.

On the analysis using the third method, only the wells with the existence of shale within the carbonates were selected. There are four wells that satisfy this requirement, they are Well B, Well E, Well G and Well I (Fig. 3.21).

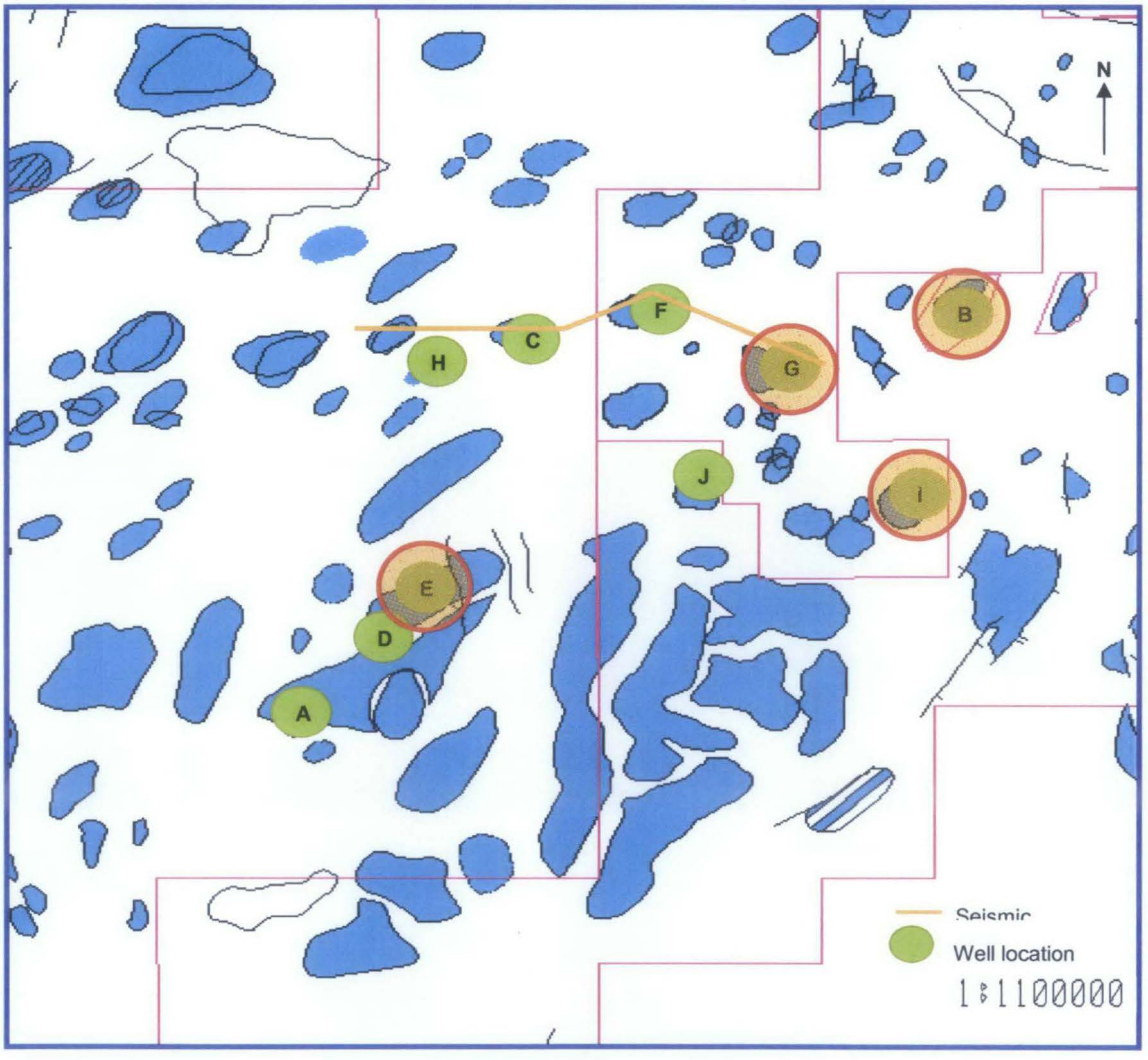

Fig 3.21 The location of the four wells selected for the Pore Pressure prediction in the carbonate section.

The visualized freehand drawn NCT was first gathered into one track and an average line representing all the NCT was drawn (Fig. 3.22). The pore pressure calculation using Eaton's equation is then performed by using the average line as the reference NCT. The outcome shows more convincing prediction of the carbonate section (Fig. 3.23). The results were illustrated in Fig. 3.23, 3.24, 3.25, and 3.26 for the well B, E, G, and I respectively. Each figure shows the comparison of Pore Prediction using NCT before average and after average.

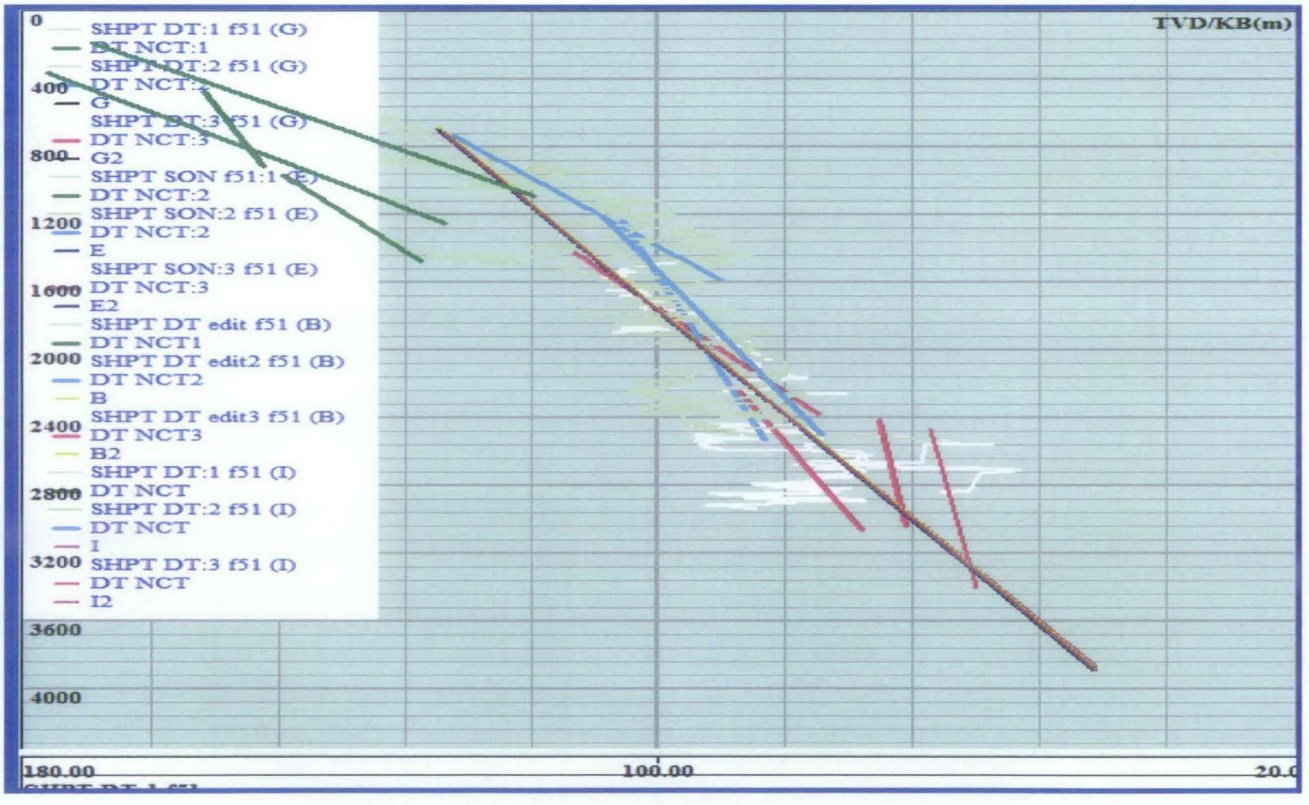

Fig. 3.22 The averaged NCT of the selected four wells.

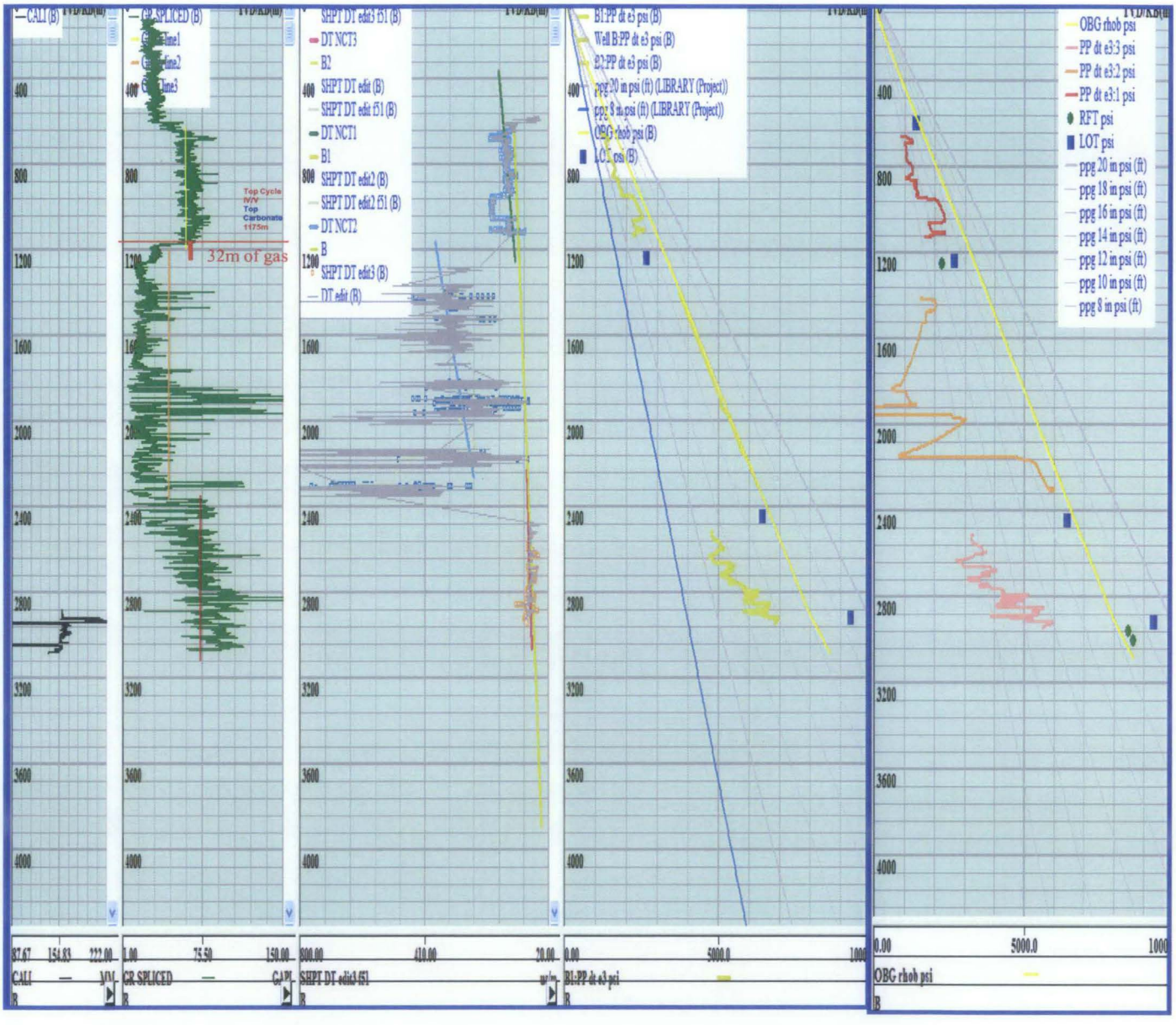

Fig. 3.23 Pore Pressure prediction using Eaton's method on Well B with comparison of different NCT used.

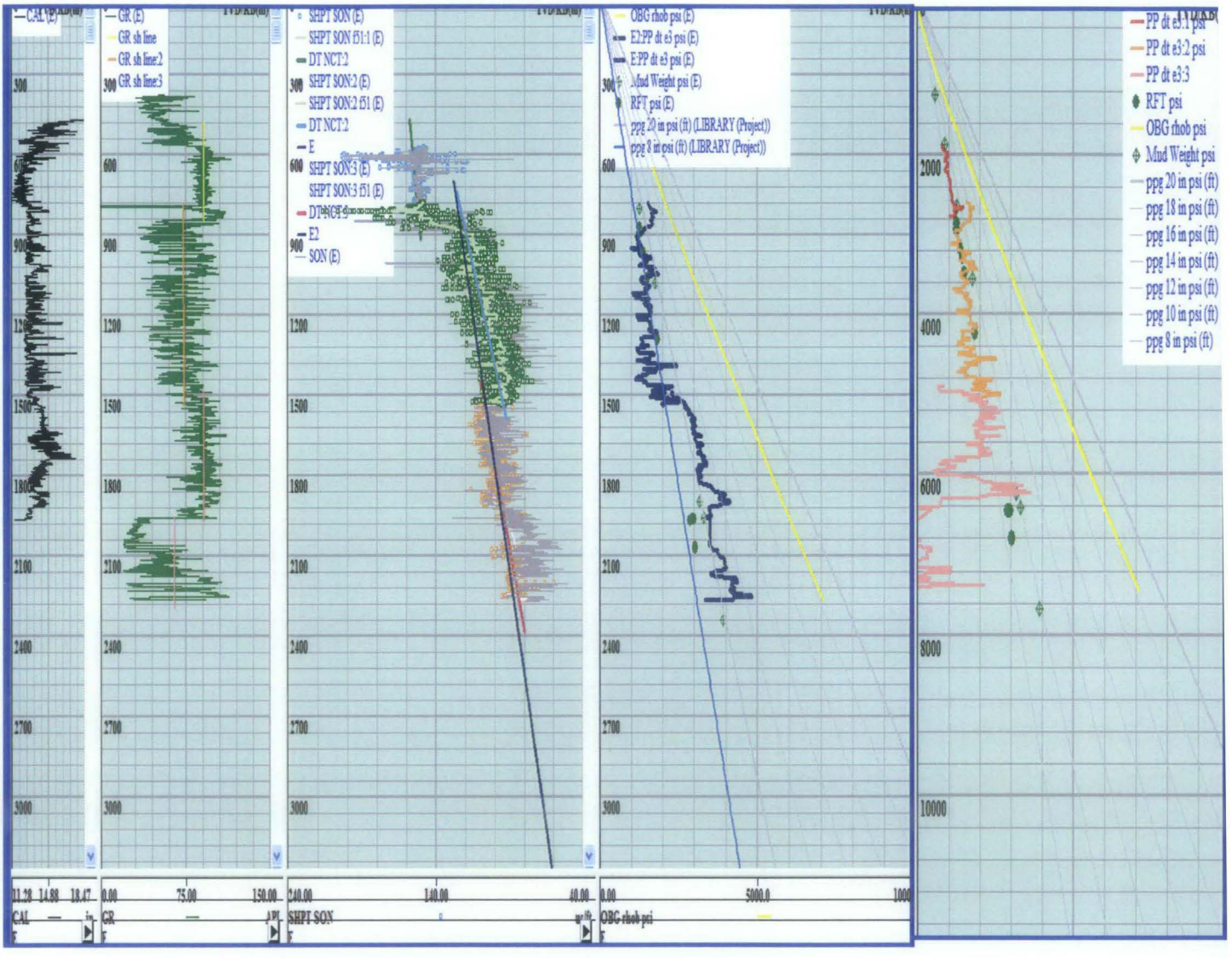

Fig. 3.24 Pore Pressure prediction using Eaton's method on Well E with comparison of different NCT used.

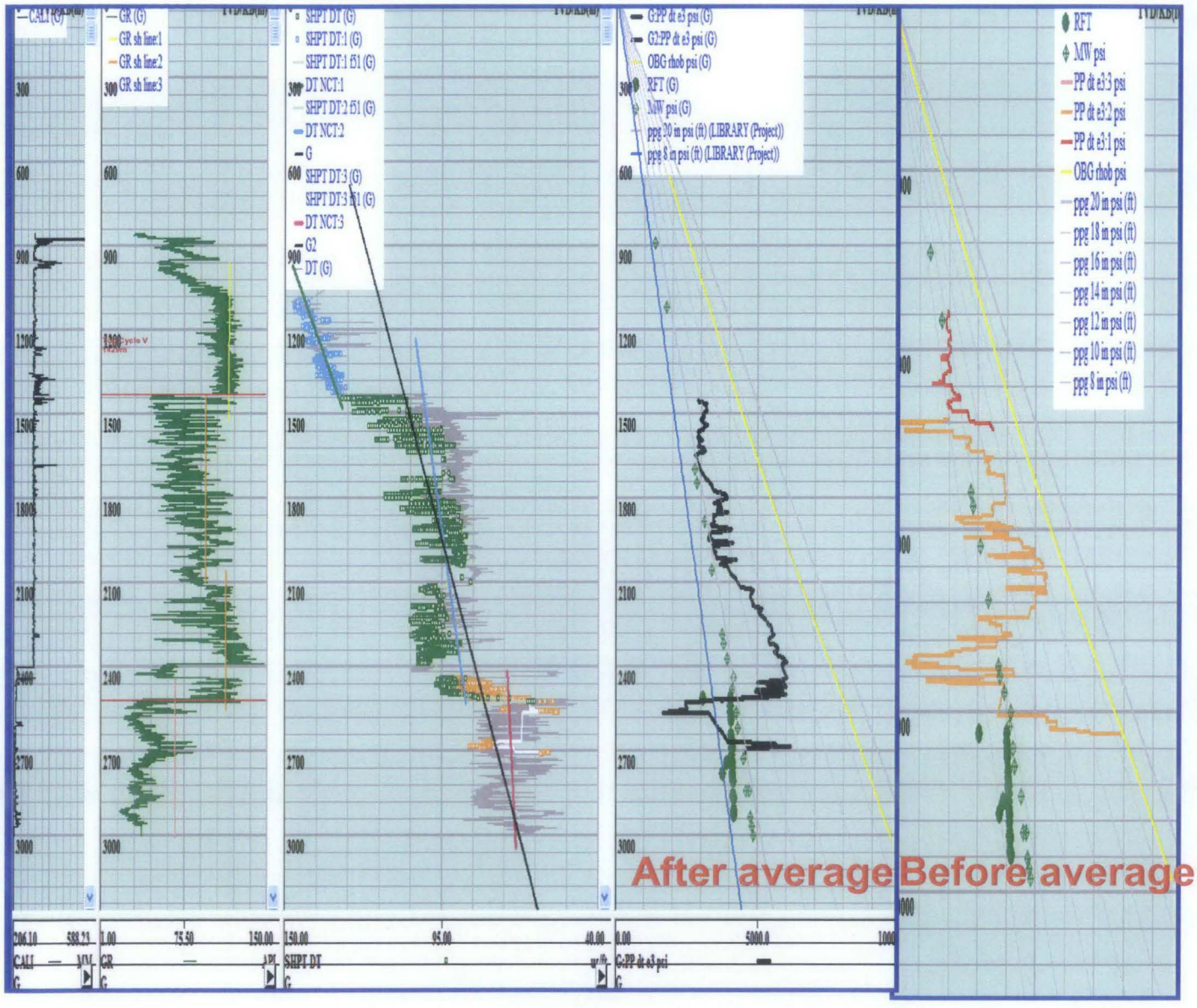

Fig. 3.25 Pore Pressure prediction using Eaton's method on Well G with comparison of different NCT used.

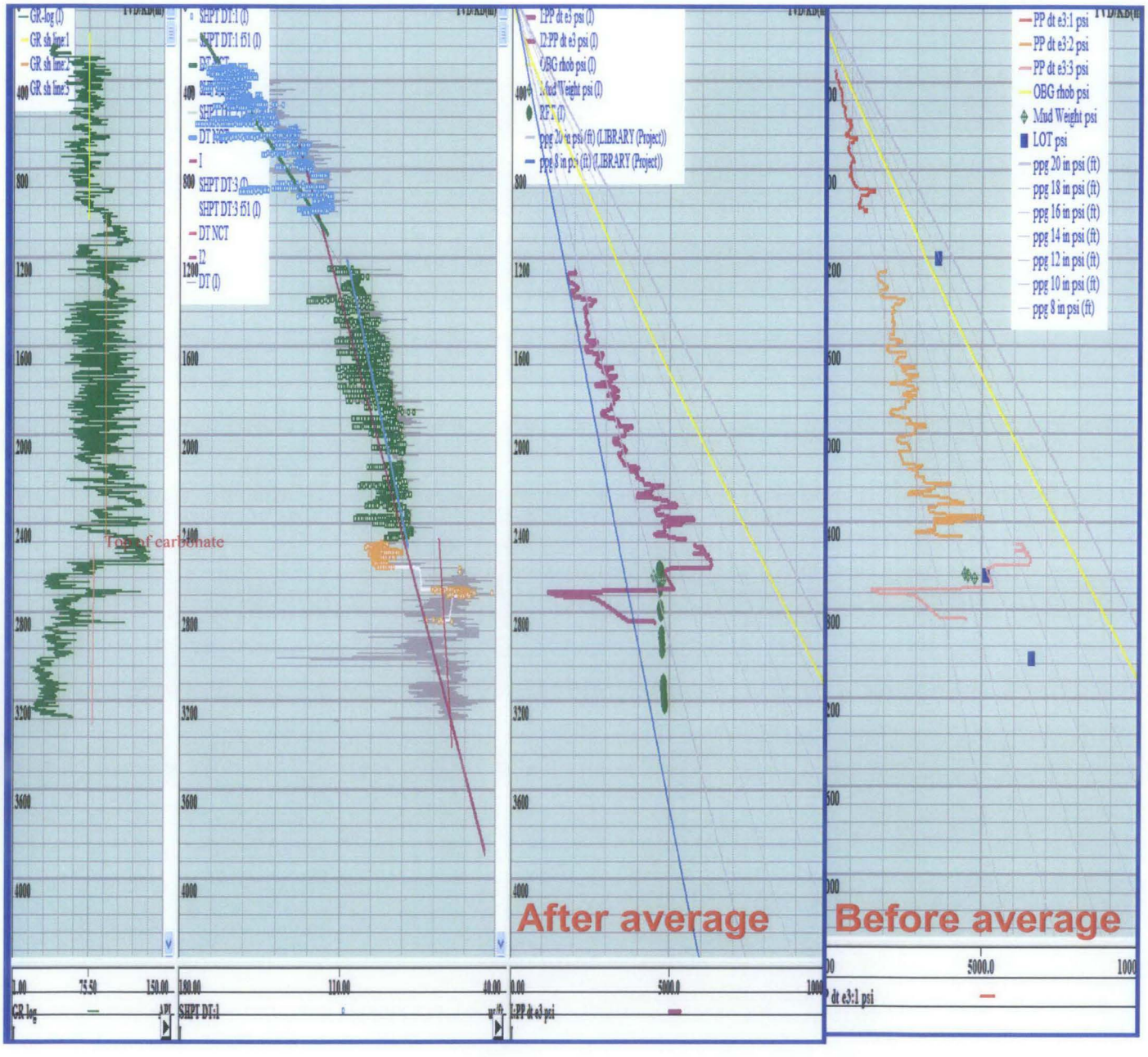

Fig. 3.26 Pore Pressure prediction using Eaton's method on Well I with comparison of different NCT used.

3.4 Summary

Ten wells were selected to represent the Eastern Central Luconia study area. These wells were selected based upon the availability of the data needed to run the Drillworks Predict software.

The gamma ray curve shows that there are several divisions occuring in the section across each wells. This division is due to the changing of lithologies. This is obvious in the changing from clastic to carbonate sequence. The other reason for the changes of the division is due to the changes in the stratigraphic unit. The changes are within the clastics itself. The changes can be seen after the top of Cycles was merged with the gamma ray curve. Due to this situation, there are three section divided according to the Gamma Ray response. The sections are the top shale section, the middle shale section and the carbonate section.

The shale points and smoothing was done on the resistivity and sonic curves. The smoothing was done using the moving weighted average (MWA) method. The number of filter points chosen was 51 for the smoothing step. 51 were chosen because, in average, it still kept the originality of the curve shape. This can easily help the interpretation of the NCT.

Over Burden Gradient was done using the density curve analysis. The compiled OBG of the ten wells shows that Well B is not in the same group with the rest of the wells. This indicates that, most probably, Well B has an overpressured regime in the deeper part of the section.

The NCT can be determined by two methods, either using the Miller's equation or using the visualized freehand drawn NCT. The NCT shows a different pattern in the top shale package and the middle shale package in both of the two methods. This difference is due to the differing of vertical loads applied for each section. The top shale section has less effect of the vertical loading because the sediment load is much lesser compared to

the middle shale section which has a thicker vertical sediment load. In the top shale section, it shows that there are large variations of facies compared to the middle shale section. In the NCT analysis, Well B seems to be outside of the group range, indicating that it has an under compacted area at the deeper part. Comparing to the OBG analysis, it shows that Well B most probably has an overpressure above the hydrostatic line scenario in the deeper part of the section.

The Pore Pressure prediction is done using three different methods involving two different equations that are Miller's and Eaton's equations. In the Eaton's equation, it involves two different curves, the resistivity and the sonic curves. In this study area, the Eaton's equation using the sonic curve is the most suitable method to do the analysis in predicting the pore pressure in the carbonate section. A total of four wells with the existence of shale within the carbonate section were chosen for the analysis. These wells are Well B, Well E, Well G and Well I.

Chapter 4:
Phase 2: Basin Modeling

4.1 Methodology

To support the study in Phase 1, basin modeling of the study area was simulated with the objective of determining the pore pressure distribution. The work flow of Phase 2 is stated as Fig. 4.1. In this phase, a few softwares were involved in the preparation prior to the basin modeling. The softwares are EZtrace, Easydepth, and Temis 2D. The first two softwares were used for digitizing and depth conversion, respectively.

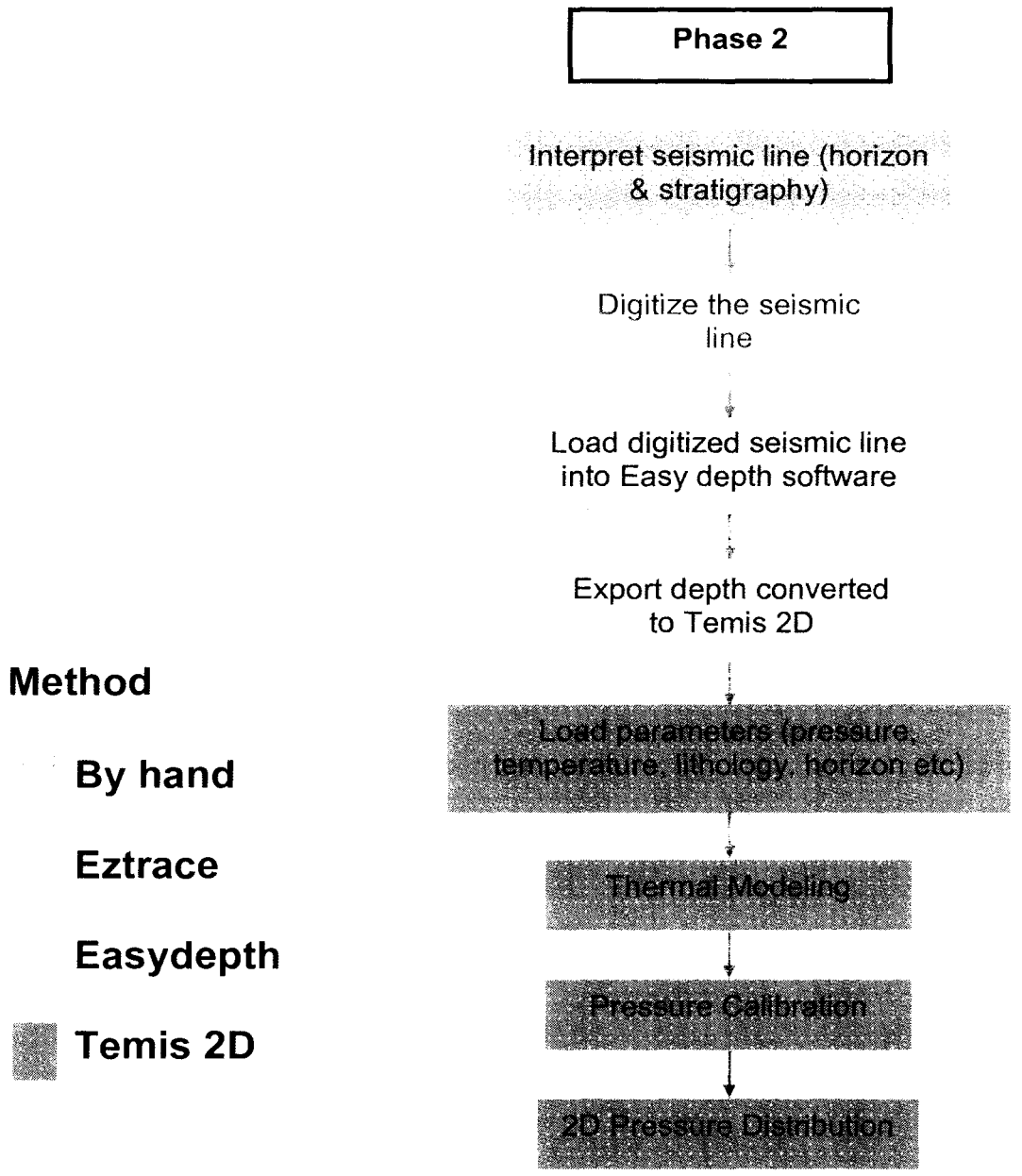

Fig. 4.1 The work flow of the Basin Modeling using the Eztrace, Easy Depth and Temis 2D software.

4.2 Data Management

During this second phase, an interpreted seismic line was needed in order to do the basin modeling. In addition, information on the well's temperature, lithology, pressure, interval velocity is also needed. A summary on the data needed is compiled in Fig. 4.2 below.

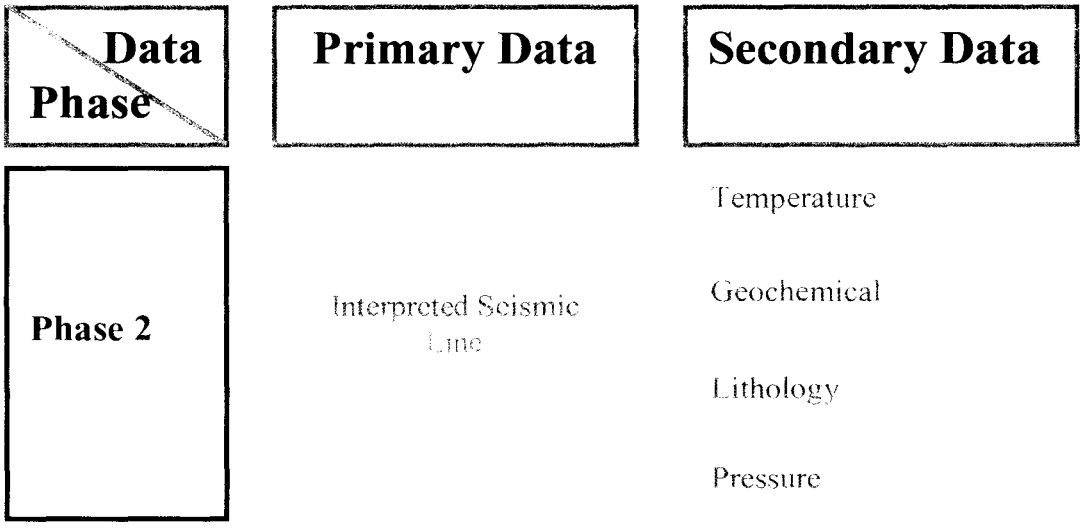

Fig. 4.2 The data needed to run the basin modeling. The primary data is the main core of the basin modeling. The secondary data is the parameter needed to run the simulation in basin modeling.

An arbitrary line (Fig. 4.3) was chosen to represent potential thief sand that was in communication with well F's carbonate buildup. This section was chosen to see the pressure evolution in the basin and how the thief sand impacts on it. This line was then interpreted, digitized and loaded into the Easy depth software to convert the time section into a depth section.

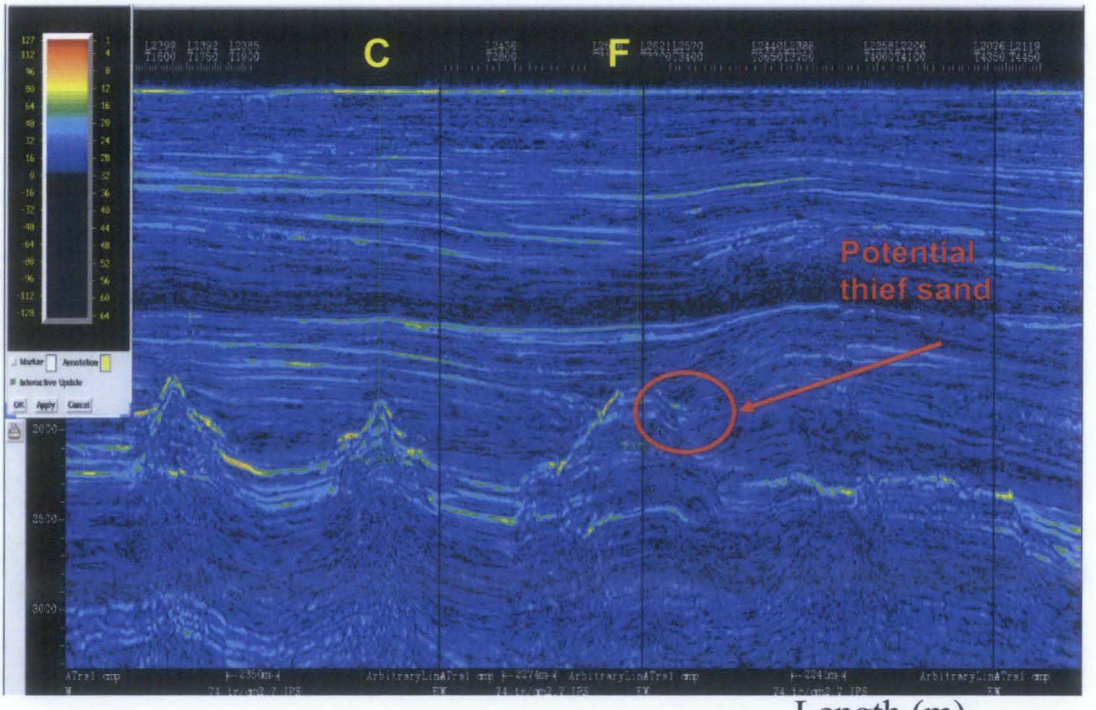

Fig 4.3 Arbitrary line showing the potential thief sand in communication with the carbonate buildup.

4.3 Data Analysis

As mentioned earlier, there are several steps involving a few softwares before we can proceed to the basin modeling study. The workflow of the study in second phase has been ilustrated in Fig. 4.1 before. In this topic, the discussion will be more on the flows involved in the basin model building stage.

4.3.1 Seismic Interpretation

A seismic line with the existence of potential thief sand has been (Fig. 4.3). The line was plotted and the interpretation was done on the hard copy using well calibrations (Fig. 4.4). Gamma ray curves were plotted to overlap with the seismic line. The changing of gamma ray signatures helps to identify different lithologies or sections. The gamma ray signatures contribute a lot to the horizon picking. The strong seismic reflector also gives a stronger interpretation. The interpreted horizons and buildups were then digitized using the EZtrace software. The digitizing steps need to be done to obtain the x and y coordinates. These x and y coordinates will be used in Easydepth software.

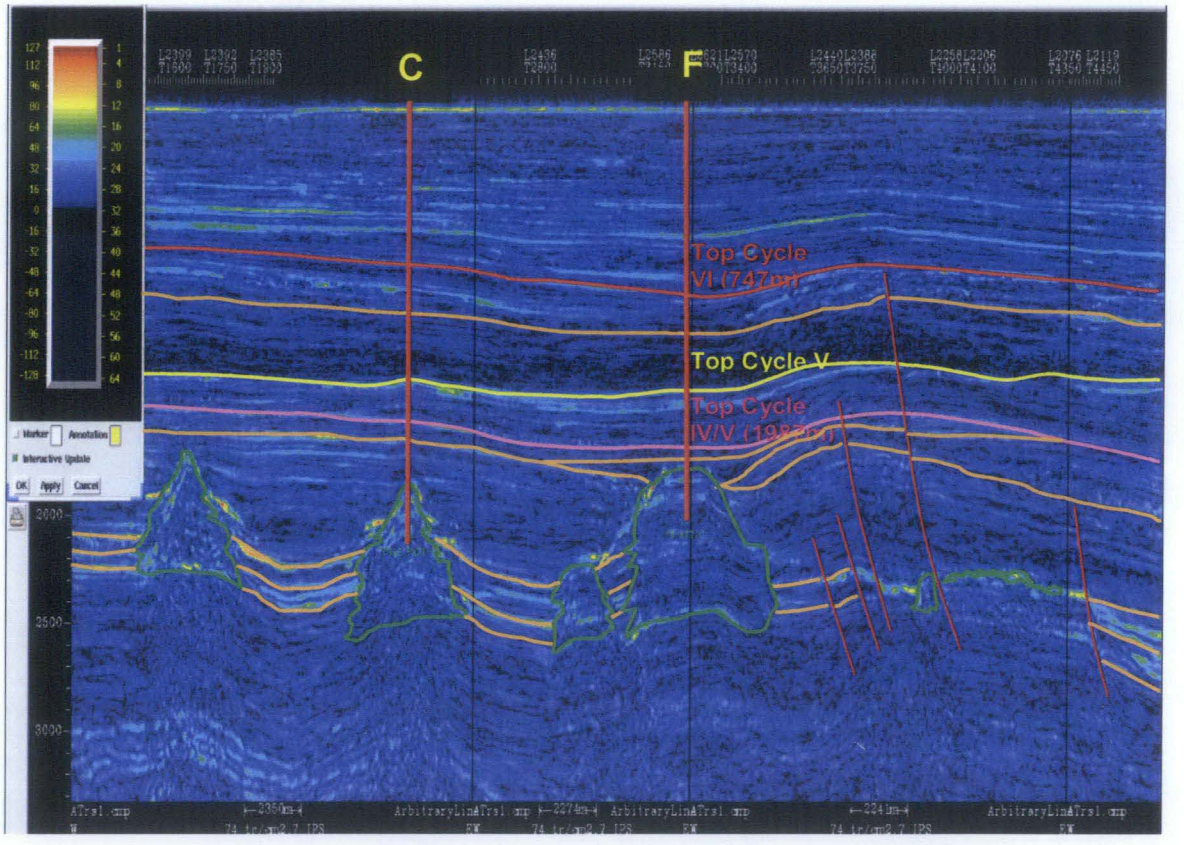

Fig. 4.4 The interpreted seismic line.

4.3.2 Easydepth

The digitized seismic section from the EZtrace software was then loaded into the Easydepth software. The aim for running this software was for the depth conversion on the time section. There are several steps before we can do the depth conversion. The workflow is illustrated in Fig. 4.5.

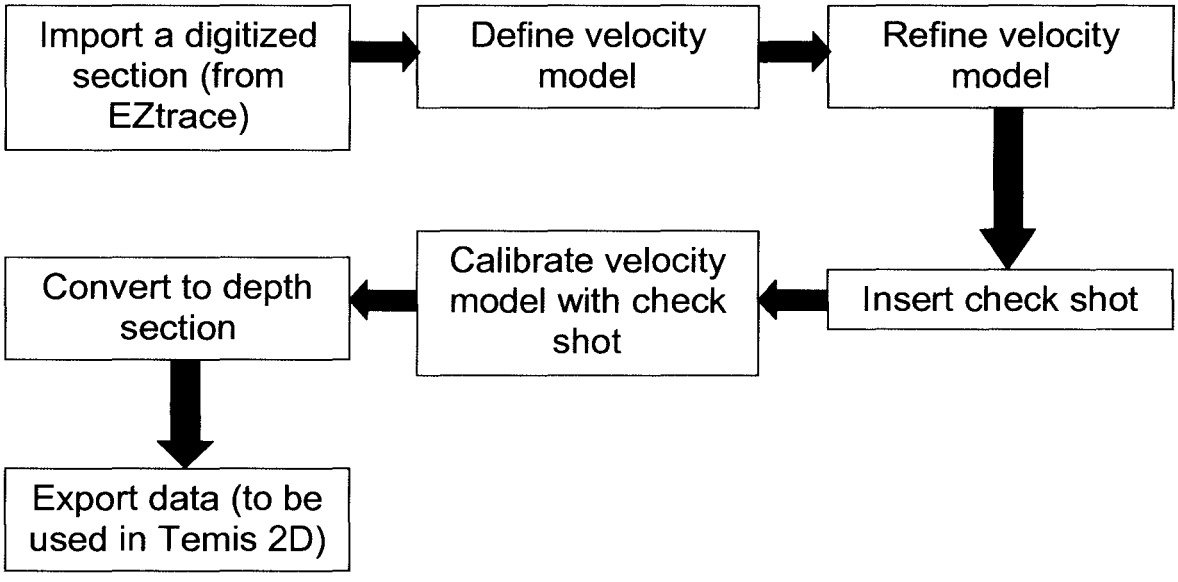

Fig. 4.5 The workflow of Easydepth.

In order to do the depth conversion, a velocity model has to be created (Fig. 4.6). The velocity model was then calibrated with the checkshot data to match the horizon depth and time. When the calibration is good, the time section can be converted to the depth section (Fig. 4.7). The depth converted section was then exported to the Temis 2D software.

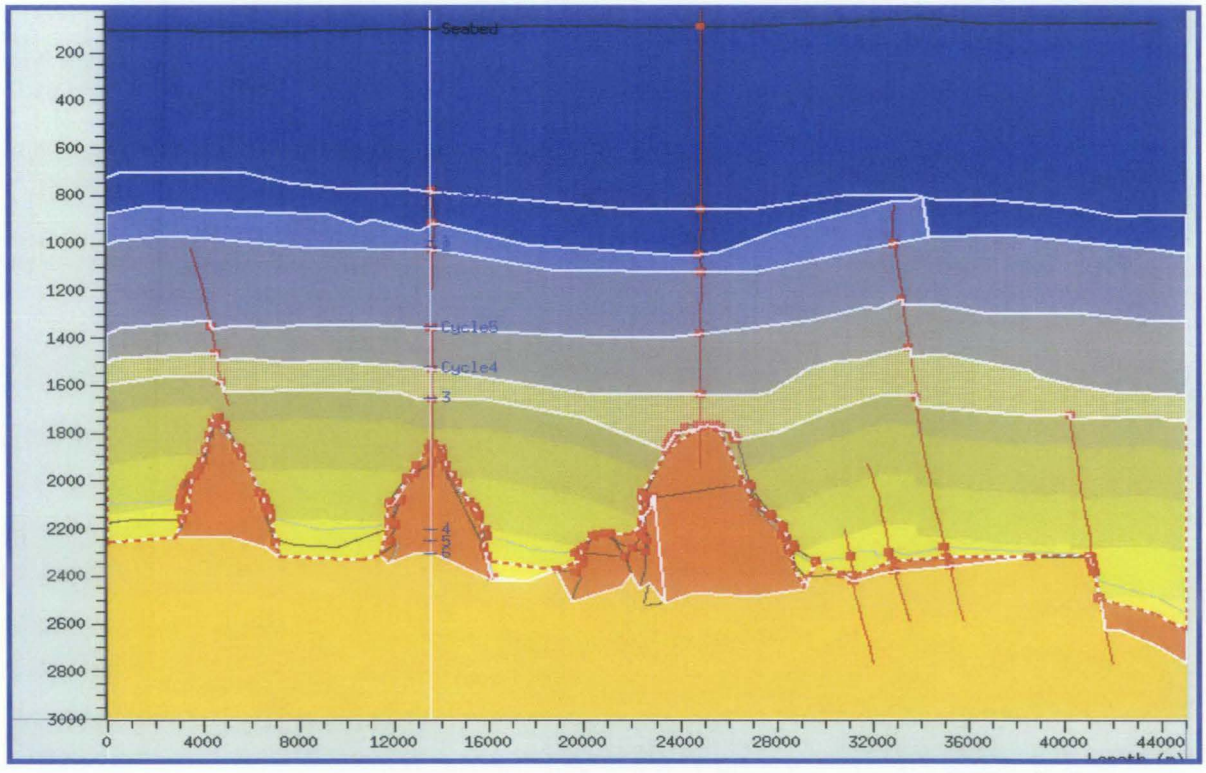

Fig. 4.6 The velocity model to enable the depth conversion process.

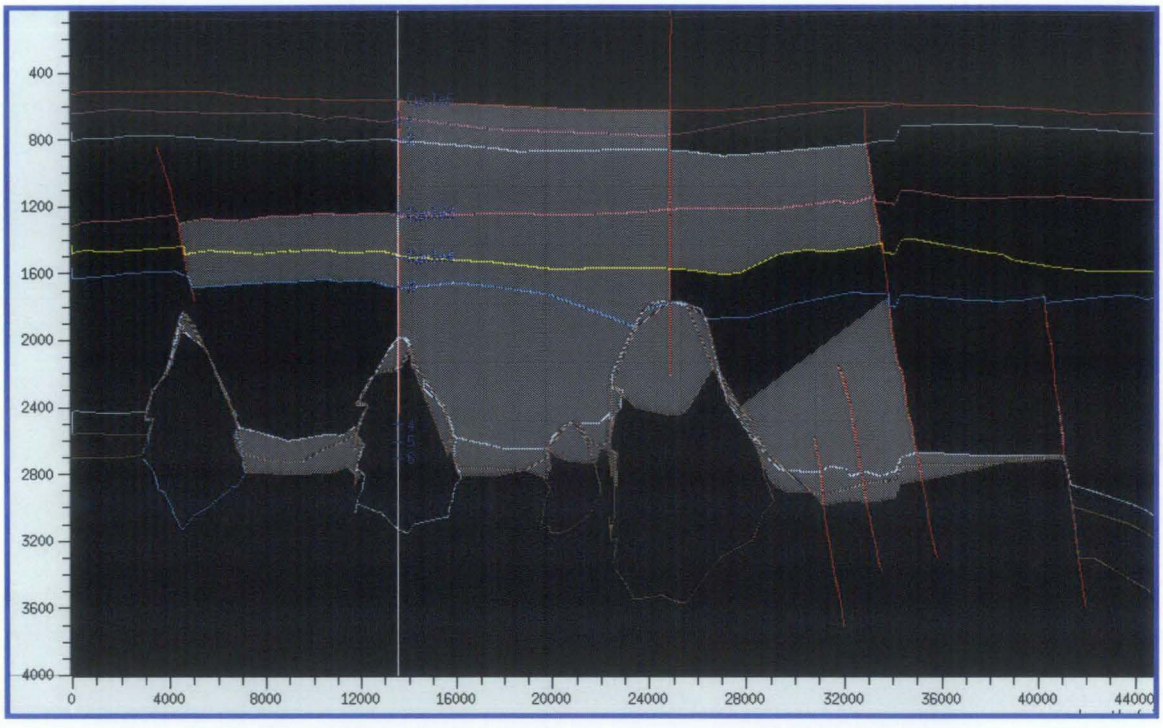

Fig. 4.7 The depth converted section.

4.3.3 Temis 2D

The data exported from Easy depth is in an .rtds2 format. The imported depth section was checked and edited to make sure the horizons remain as per the original interpretation. The section was then gridded into cells, which hold lithofacies properties. The lithology and fault was incorporated according to the geological reports and interpreted seismic line, respectively (Fig. 4.8). The cells of the section is reduced to make sure the simulation can run smoothly (Fig. 4.9). The surface temperature history, bottom temperature history, and IFP kerogens and hydrocarbon component have to be filled in order to run the simulation. After running the simulation, the model resulting from the simulation was compared with the well data, namely the temperature and the pressure data. The best fit of both simulated and well data is very crucial to make sure that the simulated model have high accuracy and closed to the real conditions (Fig. 4.10 and Fig 4.11).

Lithology	Solid Density kg/m3	Thermal Conductivity W/m/C	Spesific Surface m2/m3	Mass Heat Capacity J/kg/C
90sa+10sh	2670	5.67	200000	710
70sa+30sh	2665	4.56	2000000	740
50sa+50sh	2660	3.67	5000000	765
30sa+70sh	2650	2.95	50000000	790
shale	2645	2.37	50000000	815
carbonate 100% calcite	2710	3.57	800000	795

Table 4.1 Petrophysical properties used in the interpretation.

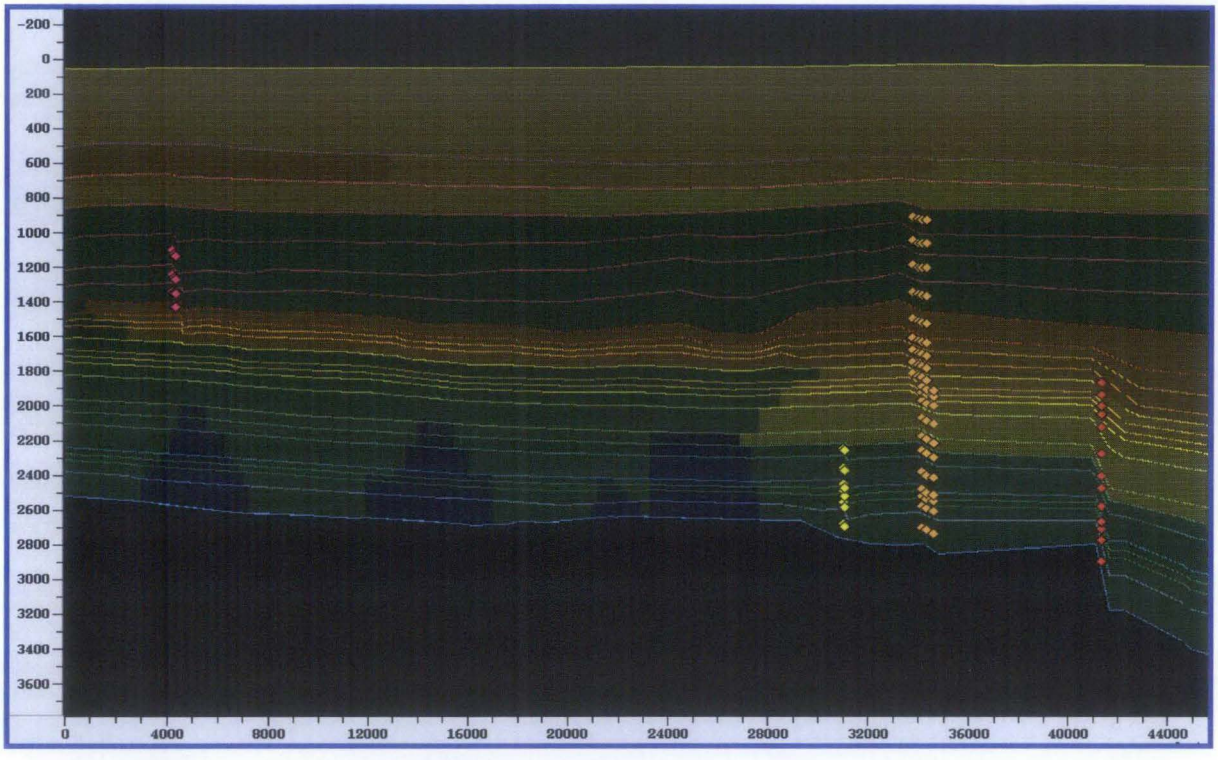

Fig 4.8 The input of lithology and fault data according to wells data of well C and well F.

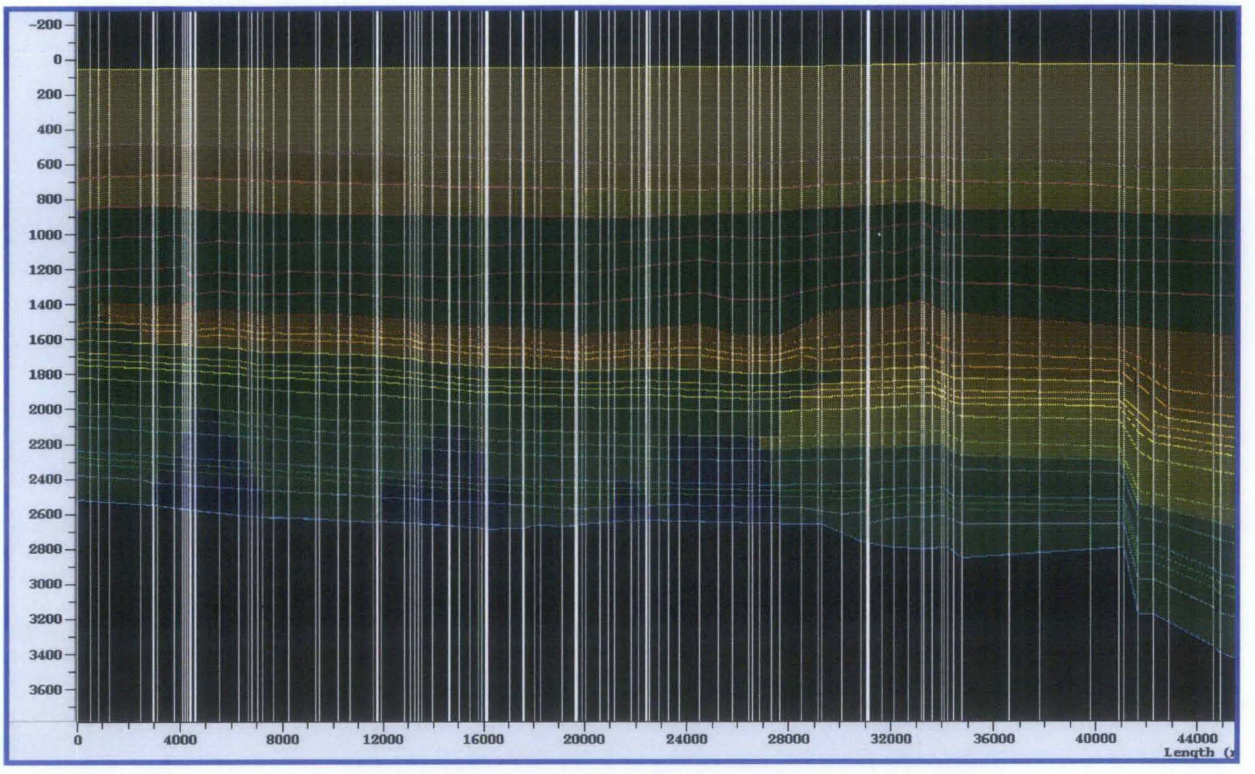

Fig. 4.9 The mesh chooses to create the cells that will be used to run simulation.

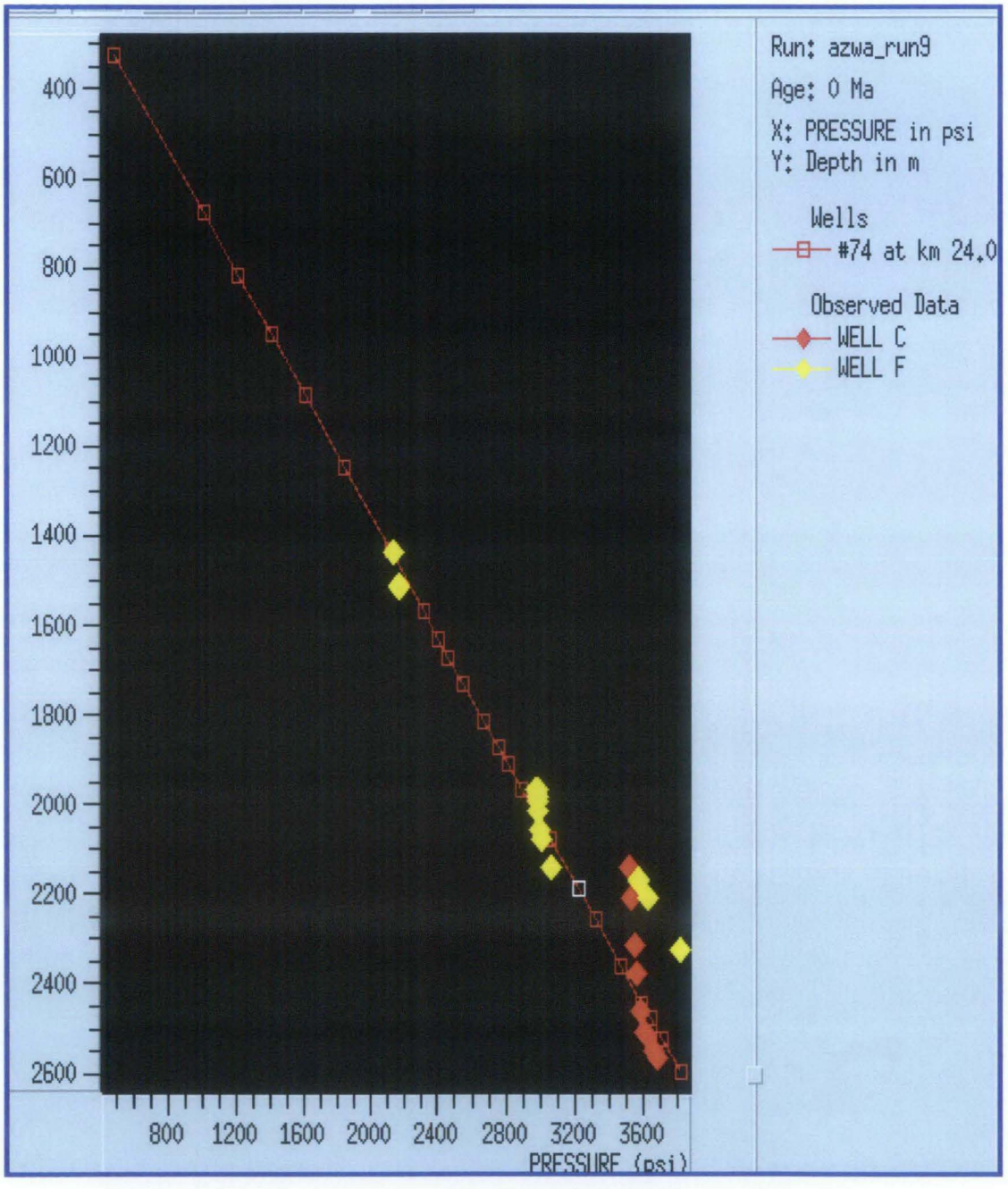

Fig. 4.10 The pressure calibration of well C and well with the simulated model. The calibration is generally good except for the well C buoyancy effect caused by the hydrocarbon column at depth of 2100m to 2400m.

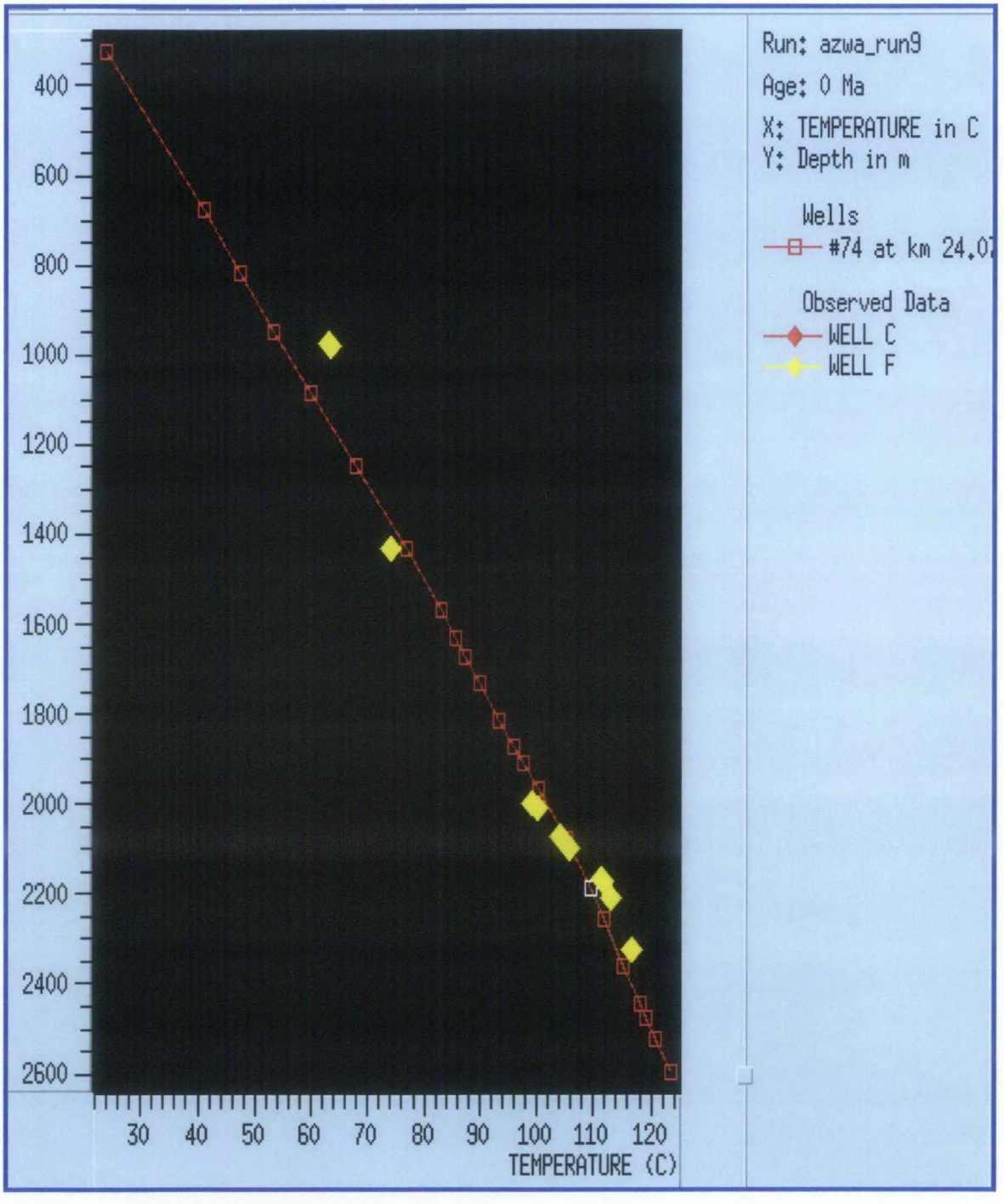

Fig. 4.11 The temperature calibration of well F with the simulated model. The calibration is good as most of the points concur with the simulated model.

4.4 Results

The simulation was done to see the pressure evolution in the basin (Fig. 4 12). The pressure starts building up when sediment load is thick enough to displace the formation water. Along with time, the sediment load is increasing due to the influx of sediment from the sediment source. The formation water will continue to be displaced as long as there is an escape route. As the sediment load is greater, compaction comes into play. The deeper sediments will be relatively more compacted than the sediments above due to the vertical loading. The compaction will reduce the size of the pore space. The remaining water that cannot escape will also be compacted, creating overpressure conditions in the pore space. In the deeper depth sections, the temperature starts to increase due to the heat flow; the increasing temperature also gave an impact to the formation water (Fig 4 .13) whereby the water will start to expand, contributing a minor pressure to the pore space.

The formation water will escape as long a there is an escape path for it to get through. The pressure will spread in a close section until it reaches equilibrium. Contact between carbonates and sand package will cause the pressure to migrate until it reaches equilibrium (Fig. 4.14). The formation water will migrate to lower pressure areas in order to transfer its pressure to get the equilibrium condition.

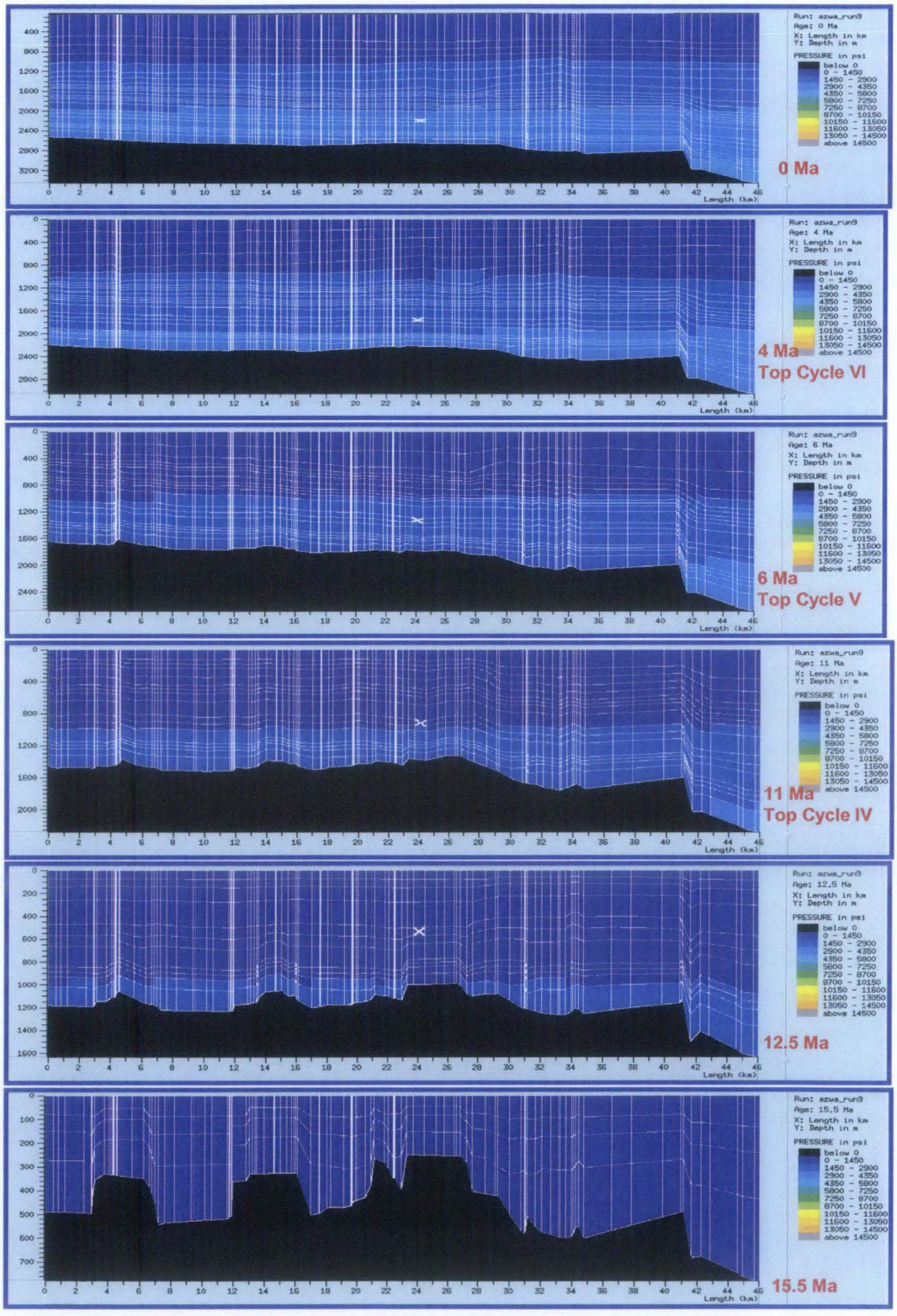

Fig. 4.12 Showing the pressure evolution through time. The pressure starts to build up when sediment load is thick enough to generate overpressure.

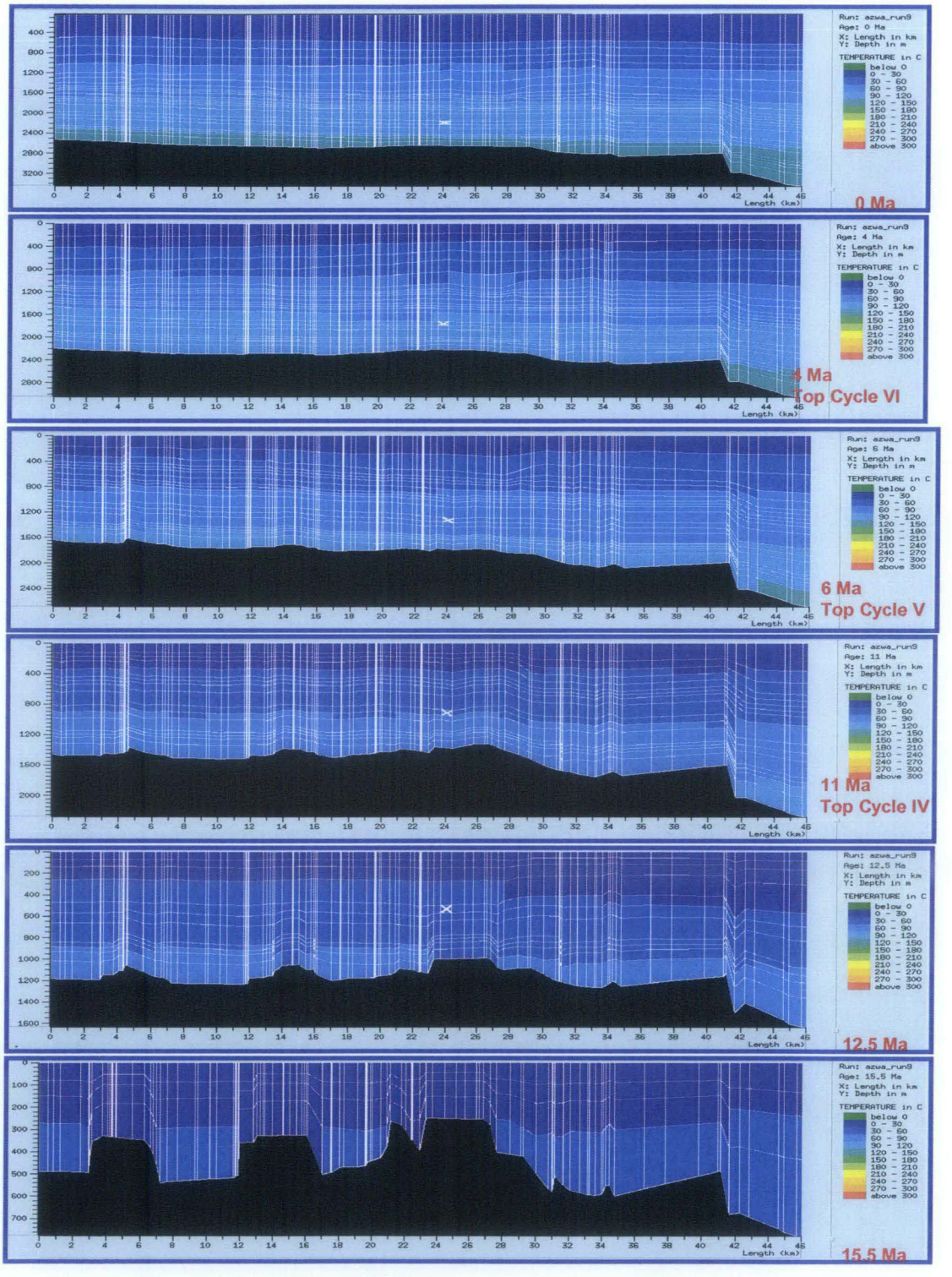

Fig. 4.13 The temperature evolution through time contributing minor pressure to the basin.

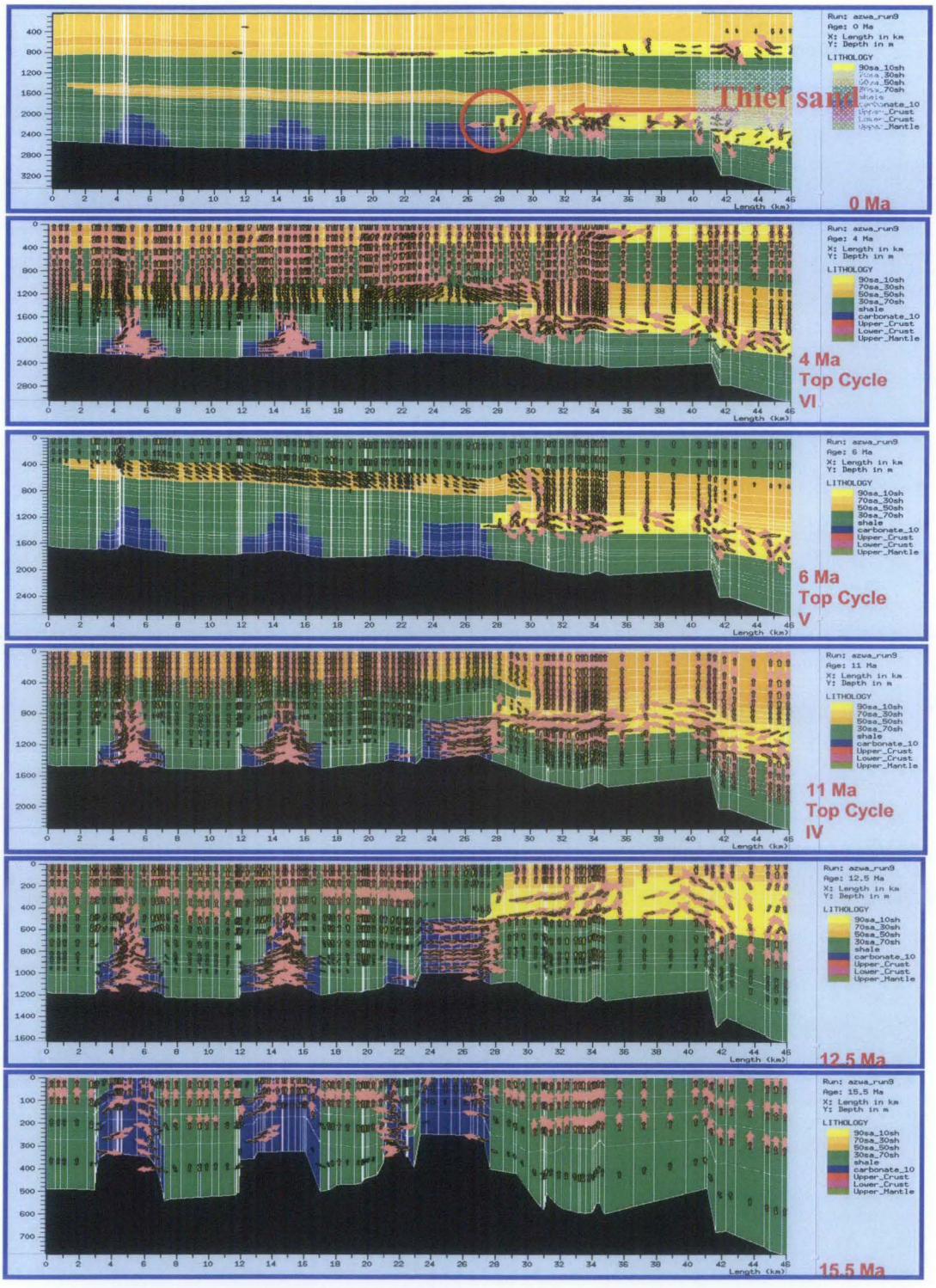

Fig. 4.14 Showing the fluid flow evolution. Water escaping from sediment leaving trapped water that cause overpressure. At 0 Ma, thief sand contributes minor pressure to the carbonate.

4.5 Summary

From the basin modeling, it shows that, apart from disequilibrium compaction as the major contributor to the overpressure in this area, there are two other minor contributors. The temperature and the fluid flow also gave a minor impact to the pressure evolution in this area.

Chapter 5:
Conclusion and Recommendation

5.1 Conclusion

5.1.1 Results

In this study area, the Eaton's calculation on sonic curve is the best method to run the wireline pore pressure prediction on carbonates. This method was used to test the overpressure caused by the disequilibrium compaction.

The main contributor of the overpressure is the disequilibrium compaction due to the sediment loading. The minor contributors are related to the fluid flow and the temperature effect.

The thief sand also gives a contribution to the pressure in carbonate as it has a higher pressure and it is trying to get to the equilibrium.

5.1.2 Recommendations

To enhance the study, it would be best if the method can be tested to some other carbonate area to further test the applicability of the method.

As for the basin modeling, the minor contributors tested were only the fluid flow and temperature. There are other contributors likely to overpressure in this area. Testing the other mechanisms, such as the impact of hydrocarbon migration, would allows to a better understanding on the pressure distribution and its evolution in this area.

References

Ali, M. Y. B., Abolins, P., 1999. Central Luconia Province. In: The Petroleum Geology and Resources of Malaysia. PETRONAS. Part 4, Chapter 15, 369-392.

Bell, D. W., (2002). Velocity Estimation for Pore-Pressure Prediction. . In Huffman. A. R. and Bowers, G. L. (eds.), Pressure regimes in sedimentary basins and their prediction: AAPG Memoir 76, p 177-215.

Bowers, G. L., and Katsube, T. J., 2002. The Role of Shale Pore Structure on the Sensitivity of Wire Line Logs to Overpressure. . In Huffman. A. R. and Bowers, G. L. (eds.), Pressure regimes in sedimentary basins and their prediction: AAPG Memoir 76, p 43-60.

Bruce, B. and Bowers, G., 2002. Pore Pressure Terminology. The Leading Edge, p. 170-173.

Burrus, J. 1998. Overpressure Models for Clastic Rocks, Their Relation to Hydrocarbon Expulsion: A Critical Reevaluation, in Law, B.E., Ulmishek G.F., Slavin V.I. eds., Abnormal Pressure in Hydrocarbon Environments: AAPG memoir 70, p. 35-63.

Dutta, N. C., (2002). Pore Pressure ahead of the Bit: An Integrated Approach. . In Huffman. A. R. and Bowers, G. L. (eds.), Pressure regimes in sedimentary basins and their prediction: AAPG Memoir 76, p 165-169.

Hennig, A et al., (2002). Pore-Pressure Estimation in an Active Thrust Region and Its Impact on Exploration and Drilling. . In Huffman. A. R. and Bowers, G. L. (eds.), Pressure regimes in sedimentary basins and their prediction: AAPG Memoir 76, p 89-105.

Hoesni, M. J. 2004. Origins of Overpressure in the Malay Basin and its Influence on Petroleum Systems. University of Durham.

Holasek, F. R., (2002). An Easily Derived Overburden Model Is Essential for the Prediction of Pore-Pressure Gradients and Fracture Gradients for Wildcat Exploration in the Gulf of Mexico. . In Huffman. A. R. and Bowers, G. L. (eds.), Pressure regimes in sedimentary basins and their prediction: AAPG Memoir 76, p 115-124.

Holbrook, P. 2002. The Primary Controls over Sediment Compaction. . In Huffman. A. R. and Bowers, G. L. (eds.), Pressure regimes in sedimentary basins and their prediction: AAPG Memoir 76, p 21-32.

Huffman, A. R., (2002). The Future of Pressure Prediction Using Geophysical Methods. . In Huffman. A. R. and Bowers, G. L. (eds.), Pressure regimes in sedimentary basins and their prediction: AAPG Memoir 76, p 217-233.

Lahann, R., (2002). Inoact of Smectite Diagenesis on Compaction Modeling and Compaction Equilibrium. . In Huffman. A. R. and Bowers, G. L. (eds.), Pressure regimes in sedimentary basins and their prediction: AAPG Memoir 76, p 61-72.

Madon, M. B. H., 1999. Basin Types, Tectono-Stratigraphic Provinces, Structural Styles. In: The Petroleum Geology and Resources of Malaysia. PETRONAS. Part 2, Chapter 5, 77-112.

Madon, M. B. H., 1999. Plate Tectoni Elemants and the Evolution of Southeast Asia. In: The Petroleum Geology and Resources of Malaysia. PETRONAS. Part 2, Chapter 4, 59-76.

Madon, M. B. H., Abd. Karim, R. B., Wong, R.H.F., 1999. Tertiary Stratigraphy and Correlation Schemes, Sequence Stratigraphy. In: The Petroleum Geology and Resources of Malaysia. PETRONAS. Part 2, Chapter 6, 113-139.

Miller, T. W., Luk, C. H., and Olgaard, D. L., 2002. The Interrelationships between Overpressure Mechanisms and In-Situ Stresses. In Huffman. A. R. and Bowers, G. L. (eds.), Pressure regimes in sedimentary basins and their prediction: AAPG Memoir 76, p 13-20.

Nguyen, T. T. B., et. al., 2007. Present-day stress and pore pressure fields in the Cuu Long and Nam Con Son Basins, offshore Vietnam. Marine and Petroleum Geology 24, p. 607-615.

Rasmus, J. C., (2002). Forward Modeling of Log Response in Geopressured Formations Reveals Vlueable Insights to the Various Pore-Pressure Prediction Techniques. . In Huffman. A. R. and Bowers, G. L. (eds.), Pressure regimes in sedimentary basins and their prediction: AAPG Memoir 76, p 159-164.

Schneider, F. and Hay, S. 2001. Compaction model for quartzose sandstones application to the Garn Formation, Haltenbanken, Mid-Norwegian Continental Shelf. Marine and Petroleum Geology 18, p 833-848.

Shaker, S. 2007. Calibrating of Geopressure Predictions using the Normal Compaction Trend: Perception and Pitfall. CSEG recorder 29, p 30-35.

Smith, M. A., (2002). Geological Controls and Variability in Pore Pressure in the Deep-Water Gulf of Mexico. . In Huffman. A. R. and Bowers, G. L. (eds.), Pressure regimes in sedimentary basins and their prediction: AAPG Memoir 76, p 107-113.

Solis et al. 2006. Normal Resistivity Trends for Geopressure Analysis in Mexican Offshore Wells. Offshore Technology Conference.

Swarbrick, R.E., Osborne, M.J., 1998. Mechanisms That Generate Abnormal Pressures: An Oveview. In Law, B.E., Ulmishek G.F., Slavin V.I. (eds), Abnormal Pressure in Hydrocarbon Environments: AAPG memoir 70, p. 13-34.

Swarbrick, R.E., Osborne, M.J., Yardley, G. S. 2002. Comparison of Overpressure Magnitude Resulting from the Main Generating Mechanisms. In Huffman. A. R. and Bowers, G. L. (eds.), Pressure regimes in sedimentary basins and their prediction: AAPG Memoir 76, p 1-12.

Tingay, M. R. P. et. al., 2002. Variation in vertical stress in the Baram Basin, Brunei: tectonic and geomechanical implications. Marine and Petroleum Geology 20, p. 1201-1212.

Yang, Y. and Aplin A. C. 2004. Defination and practical application of mudstone porosity-effective stress relationships. Petroleum Geoscience, Vol. 10, p 153-162.

Yassir, N. and Addis, M. A., (2002). Relationships between Pore Pressure and Stress in Different Tectonic Settings. . In Huffman. A. R. and Bowers, G. L. (eds.), Pressure regimes in sedimentary basins and their prediction: AAPG Memoir 76, p 79-88.

Zampetti, V. et. al. 2004. Architecture and growth history of a Miocene carbonate platform from 3D seismic reflection data; Luconia province, offshore Sarawak, Malaysia. Marine and Petroleum Geology 21, p. 517-534.

Internet references:

http://www.petrospec-technologies.com/resource/nctcalc.htm, excess on 22nd September 2007.

http://www.petrospec-technologies.com/resource/tools.htm#OBG, excess on 22nd September 2007.

http://www.otcnet.org/2006/tech_prog/sched/documents/otc181921.pdf, excess on 10th August 2007.

http://www.cseg.ca/recorder/pdf/2007/01jan/jan2007-08-geopressure-predictions.pdf, excess on 30th September 2007.

http://www.knowsys.com/uploads/PorePressureEstimationinCarbonateEnvironments.pdf, excess on 30th September 2007.

http://www.searchanddiscovery.com/documents/2005/matthews/images/matthews.pdf, excess on 30th September 2007.

Appendix A

Wells	Log Curve				Pressure Data			Check Shot
	Gr	Density	Resistivity	Sonic	MW	MDT/RFT	LOT	
A								
B								
C								
D								
E								
F								
G								
H								
I								
J								
K								
L								
M								
N								
O								
P								
Q								
R								
S								
T	Not Complete							
U								
V								
W								
X								
Y								
Z								
AA								
AB								
AC								
AD								
AE								
AF								
AG								
AH								
AI								
AJ								
AK								
AL								
AM								
AN								
AO								
AP								
AQ								
AR								
AS								
AT								
AU								
AV								
AW								
AX								
AY								
AZ								

BA								89
BB								
BC								
BD								
BE								
BF								
BG								
BH								
BI								

**** Well used in the interpretation**